CONTRIBUTION TO THE ASSESSMENT OF SHELTER-IN-PLACE EFFECTIVENESS AS A COMMUNITY PROTECTION MEASURE IN THE EVENT OF A TOXIC GAS RELEASE

María Isabel Montoya Rodríguez

A dissertation submitted in partial satisfaction of the
requirements for the degree of:

Doctor by the Universitat Politècnica de Catalunya

Supervided by:
Dra. Eulàlia Planas Cuchi

CERTEC – Centre d'Estudis del Risc Tecnològic
Departament d'Enginyeria Química
Escola Tècnica Superior d' Enginyers Industrials de Barcelona
Universitat Politécnica de Catalunya

Barcelona, September 2010

A Dios,

el creador y dador de la vida

A mis padres,

y a toda mi familia

Agradecimientos

Doy gracias especialmente a mis padres, quienes siempre me han apoyado y animado a alcanzar mis sueños, se que no ha sido fácil estar separados durante tanto tiempo por eso siempre les agradeceré el haber renunciado a sus deseos para que yo pudiera alcanzar los mios, esta tesis también es de ellos.

Gracias a todos en el CERTEC, primeramente al Dr. Joaquim Casal por permitirme hacer parte de esta familia (Elsa me encanta como le dices) y a mi directora, la Dra. Eulàlia quien sin conocerme ha puesto su confianza en mí y me ha dado la oportunidad de trabajar con ella, formarme como investigadora y crecer como persona. También a todos los profesores, Josep, Elsa, Juan Antonio, Rosa Mari y Miguel, gracias por su ejemplo, por estar pendientes de nosotros y siempre dispuestos a ayudarnos, y a Miguel nuevamente, por todas sus explicaciones y por aguantarnos. A mis compañeros, Alba, Rut, Héctor, Adriana, Yolanda, Mercedes, Diana, Jose, Miki y Ariadna, gracias por todos los momentos compartidos durante estos años. A Rut y Alba, gracias por toda su colaboración durante la parte experimental, por enseñarme la hospitalidad catalana, por escucharme y por todo el apoyo recibido en la recta final. A Héctor y Adriana, con quienes he empezado y caminado durante este tiempo gracias por estar siempre ahí de forma incondicional y a Adri, por ser esa amiga de proverbios 17:17.

También deseo agradecer a todos aquellos que me han acogido y prestado sus casas para realizar las pruebas experimentales, a Eulàlia y su familia, a Josep y Fina, a Alba y su familia, a Rut, a David y Yoli, a María, a Nuri, a Regina, a David, a Denis, a Juan Antonio y Estrella, a Pedro por toda su colaboración y a TIPS por sacarme de apuros cuando el equipo fallaba. A Rémi y

Gaëlle por haberme recibido y acogido en el CETE de Lyon durante mi estancia en Francia un gran *merci*. Junto a ellos he conocido la hospitalidad francesa. Del GBU (*Grups bíblics universitaris*), solo mencionar que mi paso por la UPC y mi vida sin su aporte jamás hubiera sido la misma, gracias por ayudarme a descubrir el verdadero sentido de la vida y por vuestra labor en la universidad.

Agradezco también al Ministerio de Educación y Ciencia, por haberme concedido una beca FPU, la cual ha sido mi sustento económico durante este periodo. Finalmente, doy gracias a Dios por cada una de las personas que ha puesto en mi camino durante este tiempo en Barcelona, pues de una u otra forma, cada una ha sido de bendición para mi vida.

Abstract

During the last decades the number of accidents in chemical industries and during transportation of hazardous substances has significantly increased, with most of them occurring in highly populated areas. One of the possible accidents is a toxic gas cloud, which although less common than other major hazards could affect larger areas reaching populated zones and producing more severe consequences. This implies then, a great challenge to emergency managers who must plan and decide the areas where protection measures should be implemented: shelter-in-place and/or evacuation. The assessment of the effectiveness of shelter-in-place is subjected to three main stages: the calculation of the outdoor gas dispersion, the estimation of indoor concentration from outdoor concentration and the evaluation of human vulnerability. This thesis is mainly focused on the study of the second stage which is primarily a function of buildings leakage.

Initially we performed a bibliographic survey with special attention on the models to estimate indoor concentration from outdoor concentration, airtightness of dwellings and ventilation models. Then, through a sensitivity analysis, we found that the air exchange rate has a great influence on the effectiveness of shelter-in-place. Moreover, since this parameter is different for each building, the knowledge of the distribution of this variable in the affected population would lead to a more accurate assessment of the effectiveness of shelter-in-place, because if we assume it as a fix value, constant for all buildings, over or underestimations of the evacuation radius may occur. Therefore, with the aim of making an estimation of the airtightness distribution in Catalunya, we applied the model developed by the Lawrence Berkeley National Laboratory (LBNL), a model based on data from North American dwellings,

to Catalan dwellings. The results obtained were influenced by climatic zones, due to the coefficients of the model, being more airtight the predictions for dwellings located in dry climates than for dwellings in humid zones. In the case of Catalunya, where constructions techniques do not differ significantly from one zone to another and most of the dwellings consist of a heavy structure, a difference such as that predicted by the model of the LBNL is not expected. Consequently, we decided to develop a model for Catalan dwellings using the air leakage database from the CETE de Lyon, since French dwellings are more likely to Catalan dwellings than US dwellings. The model developed, named the UPC-CETE model, predicts the airtightness of single-family dwellings as a function of the floor area, the age, the number of stories and the structure type: light or heavy. The airtihgtness values predicted with this model were smaller than those predicted with the model of the LBNL, as was expected.

Finally, in order to validate and improve the model developed we carried out a series of trials to measure the air exchange rate in some Catalan dwellings. Measurements in sealed rooms were also performed with the aim of assessing the reduction gained on the air exchange rate with regards to the air exchange rate of the whole dwelling. On average, we obtained reductions of 35% and found that larger reductions belonged to old dwellings with small floor areas and 1 or 2 stories. The improved model was incorporated on the methodology to assess shelter-in-place effectiveness on the stage concerning the estimation of the air exchange rate of the dwellings located on the affected zone; then, the assumption of a constant value is avoided. These measurements and the model constitute therefore the first proposal for estimating the airtightness distribution of single-family dwellings that could be used by Catalan authorities for emergency response planning.

Resumen

En los últimos años el número de accidentes en la industria química y durante el transporte de mercancías peligrosas ha aumentado substancialmente, registrándose la mayoría de ellos en zonas altamente pobladas. Las nubes de gases tóxicos suelen ser producto de estos accidentes y aunque menos probables que otros accidentes, pueden alcanzar grandes extensiones y contaminar zonas pobladas, provocando graves consecuencias. Esto conlleva un gran reto para las autoridades civiles, quienes deben evaluar y decidir el área que se debe evacuar y el área en que se debe implementar el confinamiento como medida de protección. La evaluación de la efectividad del confinamiento comprende tres etapas fundamentales: el cálculo de la dispersión exterior, el cálculo de la concentración interior en función de la concentración exterior y la evaluación de los efectos adversos sobre la salud. Esta tesis se enfoca principalmente en el estudio de la segunda etapa, la cual es función de la tasa de infiltración de aire en las edificaciones.

Inicialmente se realizó una extensa revisión bibliográfica sobre las tres etapas, haciendo énfasis en la búsqueda de modelos para el cálculo de la concentración interior, la tasa de infiltración y la hermeticidad de las viviendas. Posteriormente, a través de un análisis de sensibilidad se encontró que la tasa de renovación de aire tiene gran influencia sobre la efectividad del confinamiento, y además, dado que ésta varía para cada edificación, el conocimiento de su distribución en una población es necesario para una evaluación adecuada de la efectividad del confinamiento; ya que asumirla constante para todas las edificaciones puede llevar a sobreestimaciones o subestimaciones del radio de evacuación. Por lo tanto, con el fin de obtener una aproximación de la distribución de hermeticidad, se aplicó el modelo

desarrollado por el Lawrence Berkeley National Laboratory (LBNL), que proviene de datos de viviendas norteamericanas, a las viviendas catalanas. Sin embargo, los resultados obtenidos se encontraban sesgados a las zonas climáticas, siendo más herméticas las predicciones para viviendas ubicadas en zonas secas que en zonas húmedas, debido a los coeficientes de dicho modelo. En el caso de Catalunya, donde las técnicas constructivas no varían significativamente de una zona a otra y la mayoría de las viviendas están construidas a base de materiales pesados, no es de esperarse una diferencia tan marcada como la predicha por el modelo del LBNL. En consecuencia se decidió desarrollar un modelo para las viviendas catalanas utilizando la base de datos de tasas de infiltración de viviendas unifamiliares francesas del CETE de Lyon, ya que estas viviendas tienen mayor similitud con las viviendas catalanas que las norteamericanas. El modelo desarrollado, denominado modelo UPC-CETE, permite estimar la hermeticidad de las viviendas unifamiliares en función del área, el número de plantas, la edad y el tipo de estructura constructiva: ligera o pesada. Los valores de hermeticidad predichos con este modelo fueron menores que los obtenidos con el modelo del LBNL, como se esperaba.

Finalmente, con el objetivo de validar y mejorar el modelo desarrollado, se realizaron mediciones experimentales de tasas de renovación de aire en diversas viviendas de Catalunya y en habitaciones previamente adecuadas para utilizarse como refugios, con el fin de evaluar la reducción que se gana sobre la tasa de renovación de toda la vivienda. En promedio, se obtuvieron reducciones de un 35% y se encontró que las mayores reducciones tenían lugar en viviendas antiguas, con áreas pequeñas y 1 ó 2 plantas. El modelo UPC-CETE mejorado a partir de las pruebas experimentales, se incorporó a la metodología para evaluar la efectividad del confinamiento en la etapa de estimación de la tasa de renovación de aire, evitando asumir un valor constante para todas las viviendas y promoviendo el uso de una distribución de este parámetro por sección censal afectada.

Table of contents

List of Tables

List of Figures

Chapter 1. Introduction

"Man finds God behind every door that science is able to open"
Albert Einstein

Events like accidents in chemical plants, during the transportation of hazardous materials and terrorist attacks with chemical or biological warfare agents, although little probable, could lead to catastrophic human, environmental and economic consequences. Therefore, in order to manage situations like these it is necessary to be prepared, and to know which emergency measures must be applied. Emergency measures, however, depend on the kind and severity of the accident taking place. The major hazards with which industrial facilities are faced comprise fires, explosions and toxic releases. Fires (i.e pool fire, flash fire, jet fire) are the most common but explosions (i.e BLEVE, confined and unconfined explosion) are more significant in terms of its potential damage. Nevertheless, along the history, toxic clouds are known to have the greatest potential to kill, harm and pollute zones for weeks or months. They affect wider areas than fires or explosions, and if the released substance is highly toxic such as methyl isocyanate, catastrophes like the one occurred in Bhopal, with more than 2000 casualties and 10000 injured people could take place (Khan & Abbasi, 1999; Vílchez *et al*., 1995). Gas dispersion is commonly the final stage of most of the accidents involving hazardous materials, which could turn into a toxic cloud depending on the substances involved. Therefore, toxic clouds are not only the direct consequence of an initial release or loss of containment of hazardous substances. They could also be originated as a consequence of domino effect or from the

formation of hazardous compounds as a result of combustion, runaway reactions or unwanted reactions (Cozzani *et al*., 1998).

Statistical analysis concerning the major accidents occurred during the last century (Khan & Abbasi, 1999; Vílchez *et al*., 1995) show that almost 55% of the accidents take place in fixed installations (i.e. process plants, storage tanks, loading/unloading), 40% during transportation and 5% were miscellaneous accidents. From the accidents occurred in fixed installations 71% involved a toxic release, 4% featured a combination of fire, explosion and toxic release, while the remaining 25% concern fires and explosions (Khan & Abbasi, 1999). The most common substances involved in toxic releases are ammonia and chlorine, but other substances like phosgene, hydrogen sulphide, TCDD, methyl bromide, fungicide, hydrogen chlorine and methyl isocyanate are also found. Regarding accidents during transport, Khan and Abbasi (1999) reported that from a historical analysis including 1320 accidents, most of them occurred by rail (37%) and road transport (29%). However, according to a more recent survey of accidents by road and rail developed by Oggero *et al*. (2006), including 1932 accidents, a higher percentage of events happened in roads (63%) while a smaller one in railways (37%). Therefore the trend has changed during the last years and road accidents are more common now, which could be attributed to the increased use of this kind of transport. Oggero *et al*. (2006) also classified the accidents surveyed by type; they found that releases were the most common type of accidents (78%) followed by fires (28%), explosions (14%) and gas clouds (6%); these percentages sum up more than 100% since fires, explosions or gas clouds can follow a release in some cases.

In general, the number of accidents in chemical industries and during the transportation of hazardous substances has significantly increased since 1980, this significant increment in the number of accidents has been attributed to the improvement of access to information on accidents, to the development of industrial activity in most countries (Vílchez *et al*., 1995) and to the globalization of the chemical market. Regarding the location of the accidents, Vílchez *et al*. (1995) analyzed this feature and found that most of the accidents (66%) occurred in a highly populated zone; 12% occurred in low-populated areas and 22% in rural areas. They also reported that in 72% of the accidents people were evacuated. These results might be due to the fact that most of the industries are located near populated areas. However, this situation emphasizes the need on the planning of emergency response in the case of a severe accident involving hazardous substances. This commonly includes the qualitative and quantitative risk analysis of the industries that manage hazardous materials in certain quantities, in order to set

up the type of accidents that could take place and their extend; with the aim of establishing the intervention zones and the planning of the emergency response in each case (Renau, 2008).

In Spain 35 major chemical accidents occurred during the period comprised between 1987 and 2008, in industries regulated by the European Directive on the control of major-accident hazards involving dangerous substances, known as Seveso II Directive (Directiva 96/82/CE), being Catalunya the Autonomous Community with the highest percentage (37%) as can be seen in Figure 1.1. This situation agrees well with the fact that around 30% of the industries regulated by the Seveso II Directive are located in Catalunya (Perfil Ambiental de España, 2008). Most of the accidents reported are related with the production of chemicals (40%), specially chlorine and its derivates, the petrochemical industry (32%) and the plastic production (12%) (Perfil Ambiental de España, 2005). From these accidents 24% involved toxic emissions, 32% explosions and the remaining 44% fires, emissions or spillages. Concerning the transport of hazardous materials by road and railway, an increasing trend in the number of accidents by road within years could be observed in Figure 1.2, while accidents by railway decrease. During the period 1997-2007, a total of 93% of the accidents occurred by road while 7% by railways. These values differ with those reported by Oggero *et al*. (2006) for accidents reported in the Major Hazard Incidents Data Service (MHIDAS), which is mostly due to the high usage of road transport in Spain.

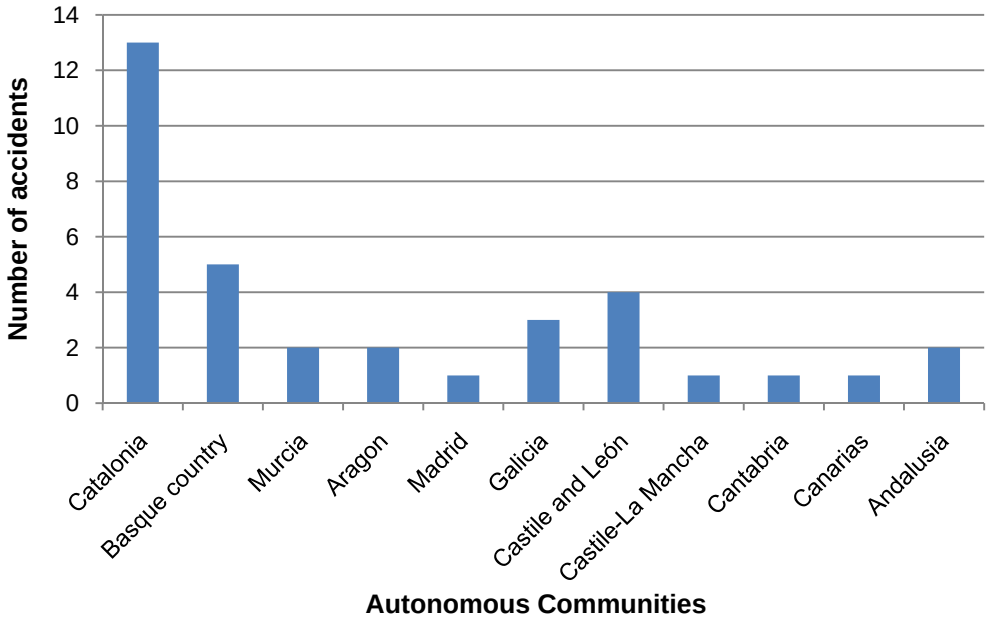

Figure 1.1 Distribution of accidents occurred in Spain from 1987 to 2008 in industries regulated by the Seveso directive distributed by Autonomous Communities

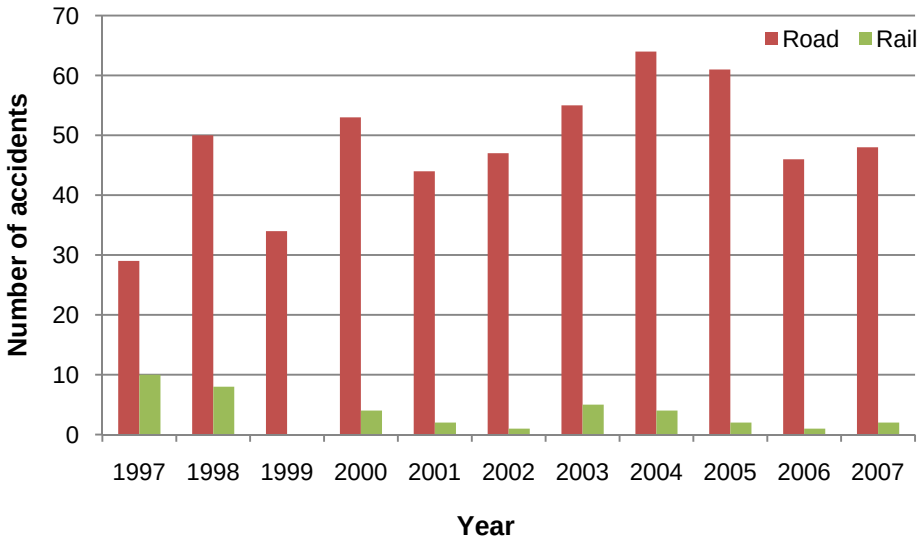

Figure 1.2 Distribution of accidents during the transportation of hazardous materials in Spain from 1997 to 2007

1.1 Toxic gas clouds and emergency response

To study the effects and consequences of a toxic gas cloud it is first necessary to compute the gas dispersion (either gaseous emission from a fixed source or vapours produced by volatile liquids spillages) in order to determine the shape of the cloud, its extend and distribution in terms of gas concentration. The dispersion involves the displacement of the gas in the wind direction and expansion in the transverse direction, both vertically and horizontally. However, the behavior of the cloud depends on the characteristics of the substance released: density, temperature, presence of droops. If the gases are diluted or its molecular weight and characteristics are similar to those of air, they are called neutral gases. This type of gases would follow the wind direction at the same height of the emission source while dispersing horizontally. By contrast, gases with a density or molecular weight higher than air and those which are at a very low temperature when released, called heavy gases, first slump and then, as they become diluted and the density of the mixture approaches that of the air, they behave as neutral gases (Dandrieux *et al.*, 2006; Carriari *et al.*, 2004). An example of a toxic gas cloud is shown in Figure 1.3, this toxic cloud took place in Cartagena (Spain) in 2002 and was the product of the spontaneous combustion of fertilizers based on nitrogen, phosphorus and potassium. Analysis performed to samples of the gas cloud revealed the presence of ammonia, nitrogenated gases and chlorine.

Figure 1.3 Toxic gas cloud in "Valle de Escombreras", Cartagena, Spain

During the dispersion of a toxic gas cloud, life and health of the people in the zone reached by the dispersion could be affected. Therefore one protection way commonly used as emergency response is to shelter-in-place, it is, to stay inside the building where you are or to go to the nearest building, close all intentional openings (i.e. windows, doors) and turn off all mechanical ventilation systems. Shelter-in-place as an emergency protection action is based on the fact that the indoor concentration will be lower than outdoors, due to the reduced ventilation rate achieved; therefore the toxic load (*TL*) to which people are exposed is lower and they could stay indoors until the toxic cloud has passed. Since most people spend the majority of their daily time inside buildings, shelter-in-place could be an easy, simple and very effective protection measure that saves money and evacuation efforts to emergency managers (Glickman & Ujihara, 1990).

In the literature there are several examples where shelter-in-place has been successfully used, some examples are shown in Table 1.1. However, a careful assessment of its effectiveness should be made to assure its applicability. Although a high reduction of the toxic load is achieved by being indoors, in some cases this reduction is not enough to keep the indoor toxic load under the toxic load limit (*TLL*), the threshold value above which any danger to life or health could occur, and therefore evacuation must be implemented. This situation usually takes place in the region nearest to the accident, where the outdoor concentration is really high and shelter-in-place does not provide a safe protection. The determination of this area is therefore of great concern to the local authorities.

Table 1.1 Accidents where shelter-in-place was implemented

Date and location	Situation	Report
May 6, 1991. Henderson, NV (US)[1]	70 tons of liquefied chlorine were released.	The people who evacuated were exposed to a higher risk of being contaminated than the people who sheltered in place.
February 7, 1993. Ludington, MI (US)[1]	Bromine was released into the air after a pipe fitting failure.	People in the area sheltered in place effectively for 3 hours.
April 6, 1991. St. Louis, MO (US)[1]	Herbicides and insecticides were released in a vapor form and as particulate matter in a fire-smoke plume.	150 local residents evacuated, while 900 prison inmates sheltered-in-place. Two injuries were reported and no fatalities.
July 16, 2003. Vallés Oriental (SP)[2]	A fire generated a toxic cloud of chlorine.	Near 100000 local residents where sheltered in place for 3 hours. The transport through railways and 2 roads was cut.
March 5, 2009. Oviedo (SP)[3]	A fire in a deposit of 500 ton of naphthalene produced a toxic cloud.	People of the towns near the incident were advised to shelter-in-place. 2 people were taken to the hospital.
January 28, 2002. Cartagena (SP)[4]. See Figure 1.3	Spontaneous combustion of fertilizers NPK generated a toxic cloud of ammonia principally. Near 15000 tons of fertilizers were involved.	14 people injured, people near industrial premises were advised to shelter-in-place.

[1] Mannan & Kilpatrick 2000
[2] http://www.belt.es/noticias/2003/julio/18/nube.htm
[3] http://www.laregioninternacional.com/noticia/47300/incendio/Qu%C3%ADmica/
[4] http://www.itfuego.com/nube_toxica_cartagena.htm

When a building is surrounded by a toxic gas cloud, and all intentional openings are closed as well as the mechanical ventilation systems are turned off, it is assumed that the gas concentration inside the building is lower than the outside concentration. Outdoor air infiltrates to the indoor space through envelope leaks, once inside, mixing with the indoor clean air takes place and the gas concentration decrease. At the same time, the toxic gas can also be retained by indoor materials increasing the reduction of the indoor concentration with respect to outdoors (Karlsson, 1994; Shair & Heitner, 1974). Thereby, one of the most important factors when assessing the effectiveness of shelter-in-place is the infiltration flow or the frequency at which the indoor air is renovated, this frequency is commonly known as the

infiltration air exchange rate or the infiltration ventilation frequency (*ACH*), and depends on the atmospheric conditions and the airtightness of the building. Several studies made in order to analyze the behavior of the *ACH* and the airtightness in residential and no residential buildings showed that there is a high variability among the buildings analyzed (Orme *et al*., 1998; Persily, 1999; Litvak *et al*., 2000a, 2000b; Angell *et al*., 2004; Sherman & Dickerhoff 1998), which generates a great difference among the degree of protection offered by each building. Therefore, the determination of shelter-in-place effectiveness in a community scale should consider the *ACH* distribution of the different buildings present in the zone, instead of assuming a constant *ACH* for all the buildings, since it could lead to under or overestimations of the evacuation area, unexpected deaths, health affections or unnecessary efforts, respectively.

Another factor to be considered in the assessment of shelter-in-place effectiveness is the non linearity of the adverse health effect, which is a function of the toxic load to which people are exposed. This toxic load depends on the concentration and exposure time, and was defined by Ten Berge (1986) as:

$$TL(t) = \int_0^t [C(t)]^n dt \qquad \text{Eq. 1.1}$$

The time of response of the population after the alarm and the moment at which shelter-in-place finish, are other factors that influence shelter-in-place effectiveness. An extended shelter, that last more than the passage time of the cloud, could expose people to equal of greater toxic loads than outdoors. Also, a delay in the implementation of shelter-in-place increase the exposure to a higher concentration and lower shelter-in-place effectiveness, as reported by Chan *et al*. (2007a & 2007b).

1.2 Catalan situation

Catalunya is a high industrialized region located in the north-eastern part of Spain which has numerous companies (180) with a high risk level according to the Seveso II Directive (PLASEQCAT, 2007). Current Spanish legislation regarding the control of severe accidents involving hazardous materials (Real Decret 1196, 2003), establish two actuation zones in the

case of a toxic gas cloud: the alert and the intervention zone. The first zone refers to the region in which accident's consequences, although perceptible by the community, does not justify intervention. The second is a zone in which those consequences generate such a level of damage that immediate protection measures must be taken. Consequently, emergency efforts ought to focus on the intervention zone and the protection measures to be taken should consider the area where shelter-in-place is effective and could be implemented. Nevertheless, previous qualitative and quantitative risk analysis of these industries should be presented (Real Decret, 1196/2003) in order to identify the scenarios that could take place and determine the possible consequences and damages, and the zone that could be potentially affected.

The alert and the intervention zones are defined based on outdoor concentration using the Acute Exposure Guidelines Levels (AEGL-1 and AEGL-2, respectively) as threshold values. If the AEGL are not available for the substance involved, the Emergency Response Planning Guidelines (ERPG-1, ERPG-2) should be used, or the Temporary Emergency Exposure Limits (TEEL-1, TEEL-2) if the ERPG are also missed (Real Decret, 1196/2003). In addition to these zones Catalan Government establishes also the evacuation zone. The criterion used to define the evacuation zone is that casualties inside buildings are higher than 0.1% (PLASEQCAT, 2007). This criterion involves the estimation of indoor concentration (C_i) and indoor toxic load (TL_i). The methodology currently used by the Catalan Government considers several factors like the substance involved, the terrain conditions, the passage time of the cloud, the arrival time of the cloud and the *ACH*, which can take a value between 2 and 5 h^{-1}. However neither experimental data concerning the *ACH* or the airtightness of Catalan buildings nor a clear methodology to establish them as a function of the building characteristics and meteorological conditions are available; consequently this value has to be assumed. Therefore, this thesis is focused on the development of a methodology to assess the effectiveness of shelter-in-place in Catalunya taking into account the estimation of the *ACH* of Catalan single-family residences depending on its characteristics, geographical location and meteorological conditions.

1.3 General scope and objectives

The main objective of this thesis is to improve the actual methodology for the assessment of shelter-in-place effectiveness in Catalunya that leads to the establishment of the zones where

shelter-in-place could be implemented as a protection measure in the case of a toxic gas release, taking into account the *ACH* distribution of the dwellings in the affected area. To attain this objective several specific objectives were also defined:

- To identify and analyze the different parameters involved in the estimation of shelter-in-place effectiveness.
- To develop a model for the estimation of the airtightness of Catalan residential building stock with the census data available.
- To assess the effectiveness of shelter-in-place in Catalunya by census tract in a geo-referenced way.
- To obtain experimental measures of the *ACH* of Catalan single-family dwellings to validate the model.

1.4 Outline of the research

This thesis is developed through seven chapters. Each chapter deals with a specific issue of the assessment of shelter-in-place in Catalunya. Following this approach, Chapter 2 presents a bibliographic survey that describes the three main stages involved in the assessment of shelter-in-place effectiveness (calculation of outdoor gas dispersion after the release, estimation of indoor concentration from outdoor concentration and evaluation of human vulnerability). The first part of Chapter 3 presents analytical expressions to calculate indoor concentration taking into account sorption processes over indoor surfaces, while the second part describes and compares the methodology used by the Catalan Government to estimate the evacuation radius, where the requirement of an accurate estimation of the *ACH* is remarked. Chapter 4 initially focuses on the analysis of Catalan single-family dwellings characteristics and their geographical distribution across Catalunya, as well as, presents average and extreme meteorological conditions. The second part shows the application of the LBNL airtightness model to estimate the *ACH* of Catalan dwellings from buildings characteristics and, average and extreme, meteorological conditions. Chapter 5 deals with the development of a statistical model to estimate the airtightness (and consequently the *ACH*) of Catalan residential dwellings, using a French air leakage database. As the best models found in

the literature came from North America, where constructions techniques, materials and climate regions significantly differ from the Catalan situation, air leakage data from French dwellings has become very useful since Catalan climate and construction techniques are more likely to the French situation. Chapter 6 presents the experimental campaign carried out to measure the *ACH* of some single-family dwellings in Catalunya and of the possible rooms that could be used as shelters under different meteorological conditions: summer and winter. Chapter 7 incorporates the estimation of the airtightness distribution of Catalan single-family dwellings obtained with the new model proposed, in the assessment of shelter-in-place effectiveness and the estimation of the evacuation radius in a geo-referenced way. Four hypothetical scenarios were analyzed in which a methodology that includes the estimation of the *ACH* distribution was proposed.

Chapter 2. Bibliographic survey

"There are no such things as applied sciences, only applications of science"
Louis Pasteur

Toxic gas clouds can be caused by a variety of events, including accidental releases on industrial premises, accidents during the transportation of hazardous materials, and attacks involving chemical warfare agents. To shelter-in-place is to take advantage of the protection offered by buildings in these kinds of situations. This protection measure is based on the fact that the building acts as a barrier that slow down the entrance of the toxic substance. Therefore, the concentration of the substance will be lower inside than outside and the toxic load to which people are exposed will be lower too (Chan *et al*., 2004; Glickman & Ujihara, 1990; Jetter & Whitfield, 2005; Karlsson, 1994; CPR 16E, 1989; Yuan, 2000). The simplest way of sheltering in place consist of closing all external openings, like doors and windows, and turning off all mechanical ventilation systems to reduce the entrance of outdoor air. This type of sheltering is known as normal sheltering. However, with the aim of improving the degree of protection offered by buildings, three additional types of sheltering had been defined by the National Institute for Chemical Studies (NICS, 2001): expedient, enhanced and pressurized sheltering. The expedient sheltering consists of taking simple measures to reduce the *ACH*, as standing in a sealed room, or sealing doors and windows with tape. The enhanced sheltering deals with the reduction of the *ACH* by making modifications to the structure, like the weatherization of homes. On the other hand, the pressurized sheltering consist of using special gas-particulate filter blower units to pressurize a sealed room or building with filtered air and, therefore, prevent polluted air from entering the shelter. Pressurized and enhanced sheltering

are the ones that offered the best protection, nevertheless, their implementation is expensive and difficult, being the normal and the expedient sheltering the most used at community level. Thereby normal sheltering is the major subject of this work.

The assessment of the effectiveness of shelter-in-place is therefore subjected to three stages: the calculation of the outdoor gas dispersion after the release, the estimation of indoor concentration from outdoor concentration and the evaluation of human vulnerability (see Figure 2.1). The first and the third stages are independent from the building, and depend on features like the release conditions or the toxicity of the substance; while the second stage depends mainly on building's airtightness, which is a function of building's characteristics. This thesis is mainly focused on the study of the second stage.

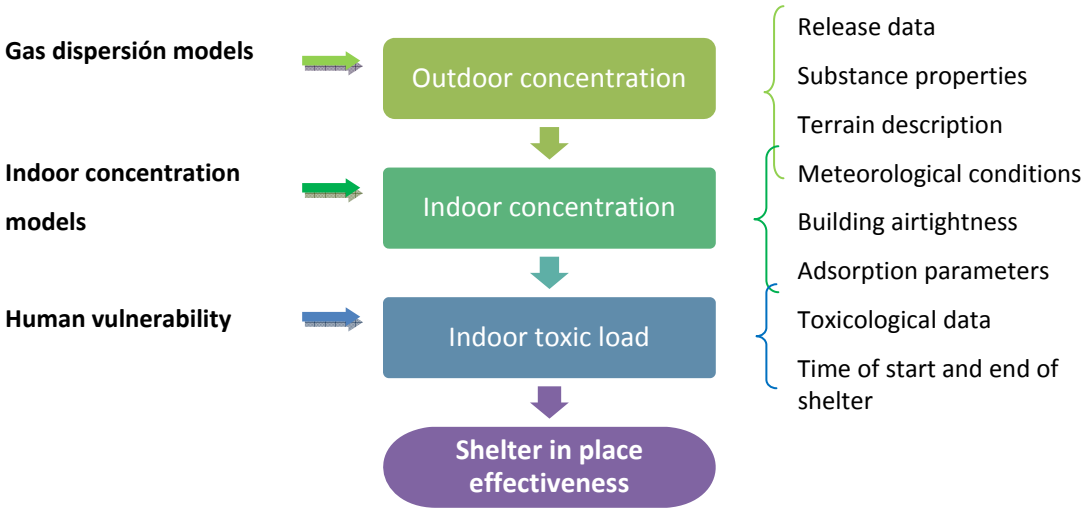

Figure 2.1 Schematic diagram of shelter-in-place assessment

In this chapter a review of the previous work concerning all the stages involved in the shelter-in-place assessment has been done.

2.1 Human vulnerability

The vulnerability of human beings against a toxic release (chemical or biological) is given by the nature of the substance and the *TL* to which people are exposed. The *TL*, as shown in Eq. 1.1,

depends on the concentration, time and toxic load exponent *n* of the substance, which is determined empirically based on animal experiments (CPR 18E, 2005). This parameter generally lies between 0.5 and 4 for toxic gases, as presented in Table 2.1 for some toxic substances.

Table 2.1 Values of *n* for some toxic substances (CPR 18E, 2005)

Substance	*n*	Substance	*n*
Acrolein	1	Hydrogen cyanide	2.4
Acrylonitrile	1.3	Hydrogen fluoride	1.5
Allylalcohol	2	Hydrogen sulfide	1.9
Ammonia	2	Methyl bromide	1.1
Azinphos-methyl	2	Methyl isocyanate	0.7
Bromine	2	Nitrogen dioxide	3.7
Carbon monoxide	1	Parathion	2
Chlorine	2.75	Phosgene	1
Ethylene oxide	1	Phosphamidon	0.7
Hydrogen chloride	1	Phosphine	2
Sulphur dioxide	2	Tetraethyllead	2

Concentration in mg/m^3, time in minutes

If the value of *n* is higher than one, the substances are known as peak chemicals since the adverse effects are increased by brief peak concentrations. In this case, shelter-in-place reduces the *TL* even when the mean indoor concentration is close to the outdoor value (Mannan & Kilpatrick, 2000). Other kind of toxic substances are the cumulative chemicals, which are more harmful when exposure is for extended periods of time at any concentration, such as methyl isocyanate. For this type of substances shelter-in-place would provide a good protection only in cases where the concentration is low and the exposure time is short (Mannan & Kilpatrick, 2000). Finally the most toxic substances are classified as immediate dosage chemicals, which are harmful at any concentration with one exposure, such as the nerve agents (i.e. sarin, VX).

When the *TL* exceeds some threshold exposure values, certain health affections or even casualties could take place, depending on the threshold level. These thresholds are known as the toxic load limits *TLL* and are estimated using the toxic levels of concern (LOCs) or percentage of casualties. There are several LOCs already defined and commonly used like the Acute Exposure Guideline Levels (AEGL), the Emergency Response Planning Guidelines (ERPG), the Immediately Dangerous to Life or Health (IDHL) and the Temporary Emergency Exposure

Limits (TEEL) among others. In general, these LOCs establish a threshold concentration for a given exposure time, above which people could start to experience adverse health effects. Currently, the AEGL, developed by the US Environmental Protection Agency (EPA), are the LOCs that most resemble to a short exposure since they intend to describe the risk to humans resulting from once-in-a-lifetime, or rare, exposure to airborne chemicals (EPA, 2009). The AEGL comprises three degrees of severity of toxic effects (AEGL-1, AEGL-2 and AEGL-3) applicable to emergency exposure periods ranging from 10 minutes to 8 hours (10 and 30 minutes, 1 hour, 4 hours, and 8 hours). It is believed that these LOCs are applicable to the general population including infants and children, and other individuals who may be susceptible. The three AEGLs have been defined as follows (EPA, 2009):

AEGL-1 is the airborne concentration, expressed as parts per million or milligrams per cubic meter (ppm or mg/m^3) of a substance above which it is predicted that the general population, including susceptible individuals, could experience notable discomfort, irritation, or certain asymptomatic non sensory effects. However, the effects are not disabling and are transient and reversible upon cessation of exposure.

AEGL-2 is the airborne concentration (expressed as ppm or mg/m^3) of a substance above which it is predicted that the general population, including susceptible individuals, could experience irreversible or other serious, long-lasting adverse health effects or an impaired ability to escape.

AEGL-3 is the airborne concentration (expressed as ppm or mg/m^3) of a substance above which it is predicted that the general population, including susceptible individuals, could experience life-threatening health effects or death.

Therefore, the *TLL* could be established through Eq. 1.1 using the LOC as the concentration for the time it has been defined, as shown in Eq. 2.1.

$$TLL = \int_0^t [LOC]^n \, dt \qquad \text{Eq. 2.1}$$

When the threshold defined involves a given percentage of casualties instead of a threshold concentration for a given exposure time, the estimation of the *TLL* is then commonly performed using the vulnerability analysis proposed by the Netherlands Organization for Applied Scientific Research (CPR 18E, 2005). This vulnerability analysis uses the Probit

functions to calculate the probability of deaths (Eq. 2.2 and Eq. 2.3). These functions relate the magnitude of the incident with the damage caused. In the case of a toxic gas release, the magnitude of the incident is the *TL* received by the people exposed (Eq. 1.1). This magnitude is used to calculate the Probit variable (P_r) and then the casualties' probability (P).

$$P_r = a + b \cdot \ln(TL) \qquad \text{Eq. 2.2}$$

$$P = \frac{1}{2}\left[1 + erf\left(\frac{P_r - 5}{\sqrt{2}}\right)\right] \qquad \text{Eq. 2.3}$$

In these equations a, b and n are constants that depends on the substance (CPR 18E, 2005). The *TLL* for a given percentage of casualties is therefore:

$$TLL = \exp\left(\frac{P_r - a}{b}\right) \qquad \text{Eq. 2.4}$$

2.1.1 Shelter-in-place effectiveness indicators

To assess shelter-in-place effectiveness there are different types of indicators. Ones are used to calculate the *TL* reduction gained by being indoors, others evaluate if the *TLL* is exceeded, and finally others relate the population both inside and outside the shelters, where the *TL* is exceeded. The first ones comprise the protection factor (*PF*), the toxic load reduction factor (*TLRF*) and the safety factor multiplier (*SFM*), from which the *PF* and the *TLRF* are the oldest indicators used to assess the effectiveness of shelter-in-place (CPR 16E, 1989; Blewett & Arca, 1999; Mannan & Kilpatrick, 2000; Jetter & Whitfield, 2005). The second ones include the safety factors (*SF*) and the last one the casualties reduction factor (*CRF*).

The *PF* is defined as the ratio of the cumulative exposure outdoor over the cumulative exposure indoors, being the cumulative exposure the lineal integration of the concentration over time, as shown in Eq. 2.5. This indicator has been mainly used for the assessment of expedient sheltering (Blewett & Arca, 1999; Jetter & Whitfield, 2005; Jetter & Proffitt, 2006). The drawback of the *PF* is that it neglects the non linearity of the exposure.

$$PF(t) = \frac{\int_0^t C_o dt}{\int_0^t C_i dt} \qquad \text{Eq. 2.5}$$

The *TLRF* relates the *TL* perceived indoors (TL_i) with the *TL* that is perceived outside (TL_o). As shown in Eq. 2.6, this indicator represent the fraction of the TL_o that is avoided by being indoors, nevertheless a high reduction does not imply a safe shelter since the TL_i could be greater than the *TLL*. A *TLRF* near 1, means that a good reduction of the *TL* is achieved (even if the *TLL* is exceeded), while a value near 0 means an ineffective shelter.

$$TLRF(t) = \frac{\int_0^t {C_o}^n dt - \int_0^t {C_i}^n dt}{\int_0^t {C_o}^n dt} = 1 - \frac{TL_i}{TL_o} \qquad \text{Eq. 2.6}$$

The *SF* represents the constant by which the exposure concentration can be multiplied without exceeding the *TLL* (Chan *et al*., 2007a). As presented in Eq. 2.7 and Eq. 2.8, it relates the *TL* (indoor or outdoor) with the *TLL*. This indicator gives a general idea of the situation in each one of the affected zones, a value under 1 means that the *TL* perceived is greater than the *TLL* and thus shelter-in-place does not represent a good protection measure, while higher values represent better protection.

$$\int_0^t [SF * C(t)]^n dt = TLL \qquad \text{Eq. 2.7}$$

$$SF = \left[\frac{TLL}{TL(t)}\right]^{\frac{1}{n}} \qquad \text{Eq. 2.8}$$

The *SFM* represents the relation between the indoor and outdoor safety factors (Eq. 2.9 and Eq. 2.10), the increment on the SF_i gained by shelter-in-place with respect to the SF_o (Chan *et al*., 2007a). A high value of the *SFM* indicates an effective shelter while a value approaching 1 means that no protection is gained by being indoors.

$$SF_i = SFM \cdot SF_o \qquad \text{Eq. 2.9}$$

$$SFM = \left(\frac{TL_o}{TL_i}\right)^{\frac{1}{n}} \qquad \text{Eq. 2.10}$$

The CRF represents the fraction of the population that is protected by being indoors. As shown in Eq. 2.11, it relates the population where the TLL is exceeded indoors with the population

where the *TLL* is exceeded outdoors. A value of 1 means that all the population is protected by being indoors, while a value near 0 means an inefficient sheltering, unable to provide a good protection.

$$CRF = 1 - \frac{Population \ \left(TL_i > TLL\right)}{Population \ \left(TL_o > TLL\right)} \qquad \text{Eq. 2.11}$$

2.2 Models to estimate indoor concentration

Indoor concentration models were originally developed as a mean of estimating the indoor concentration of common pollutants that affect indoor air quality (i.e. CO2, ozone, VOCs, etc). These models are based on a mass balance that assumes perfect mixing between fresh and inside air (Shair & Heitner, 1974). This approach implies a homogeneous concentration distribution within the zone, low internal resistance to airflow (i.e. few internal partitions), uniform temperature and low or null momentum effects (i.e. infiltration through small openings, no mechanical ventilation systems). As shown in Figure 2.2, the most complex case considers pollutants entering along with air due to infiltration and mechanical ventilation; these pollutants could be partly retained using filters, and once inside the building they could be eliminated through adsorption and/or diffusion into various materials. Several approaches have combined simple models that consider neither filtration nor adsorption (Jetter & Whitfield, 2005) with more complex models that consider internal and external filtration, adsorption and desorption onto surfaces, and internal diffusion into materials (Jørgensen *et al*., 2000). These models can be classified into four categories:

- With neither adsorption nor filtration.
- With filtration and constant adsorption, without desorption.
- With filtration plus variable adsorption/desorption.
- With filtration plus variable adsorption/desorption and internal diffusion.

In the first case, indoor concentration would only be lower than the outdoor concentration by an interval of time equivalent to the inverse of the *ACH*. In the other cases, the models find lower concentrations because they take into account adsorption on materials and filtration factors (mainly if the air is recycled) (Casal *et al*., 1999b; Karlsson, 1994; Yuan, 2000).

Nevertheless, desorption causes a residual indoor gas concentration over an extended period of time, which causes the indoor concentration to increase and approach the outdoor concentration if the space is not adequately ventilated after the toxic gas plume has passed (Karlsson & Huber, 1996).

All these models can be represented by a general model based on the one proposed by Shair and Heitner (1974), with the appropriate simplifications applied to each case. Thus, the general mass balance (Figure 2.2) can be expressed as follows:

$$V\frac{dC_i}{dt} = Q\cdot C_o + Q_3\cdot C_o\cdot(1-f_o) + Q_2\cdot C_i\cdot(1-f_i) - Q_2\cdot C_i - Q_1C_i - R + S \qquad \text{Eq. 2.12}$$

Combining the third and fourth terms of this mass balance, and dividing by the total volume, the following expression is obtained:

$$\frac{dC_i}{dt} = ACH\cdot C_o + ACH_3\cdot C_o\cdot(1-f_o) - ACH_2\cdot C_i\cdot f_i - ACH_1\cdot C_i - \frac{R}{V} + \frac{S}{V} \qquad \text{Eq. 2.13}$$

where ACH_j is the air exchange rate:

$$ACH_j = \frac{Q_j}{V} \qquad j = 1,2,3 \qquad \text{Eq. 2.14}$$

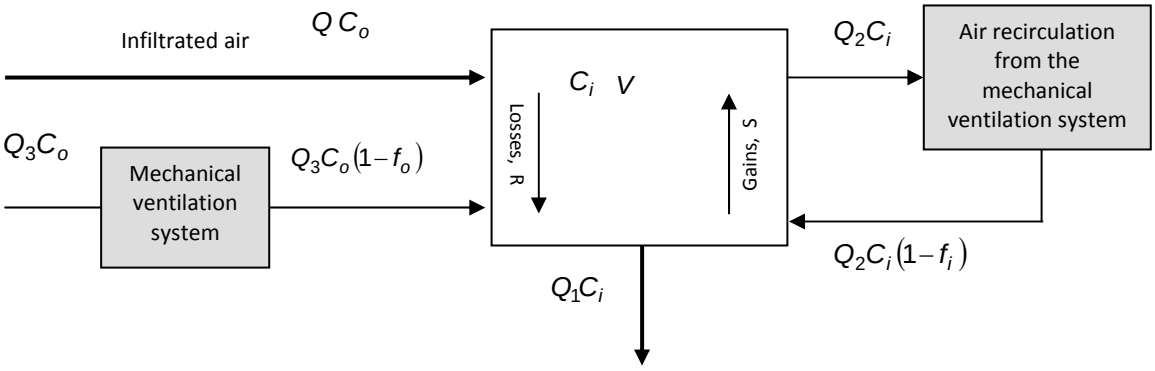

Figure 2.2 Schematic diagram of the general ventilation model.

2.2.1 Filtration parameter

Filtration usually refers to the filters of the mechanical ventilation systems through which make-up air and recycled air pass. The external filtration factor, f_o, is the fraction of pollutant in the make-up air that is retained by the filter. In addition to the fraction of pollutant retained by the filter during the recirculation of air, the internal filtration factor may also consider the pollutant fraction retained by the lungs (Karlsson, 1994; Shair & Heitner, 1974), even though this is a very small fraction that is usually neglected. As a result, only filtration due to mechanical ventilation is considered, and since most ventilation systems use the same filter for make-up and recycled air, the internal and external filtration factors are usually the same ($f_o = f_i = f$).

In the event of sheltering, it is assumed that all mechanical ventilation systems are turned off ($ACH_2 = ACH_3 = 0$) in order to reduce the entrance of toxic gas. Thus, infiltration becomes the only ventilation path ($ACH = ACH_1$). With these simplifications, Eq. 2.12 reduces to Eq. 2.15:

$$\frac{dC_i}{dt} = ACH \cdot C_o - ACH \cdot C_i - \frac{R}{V} + \frac{S}{V} \qquad \text{Eq. 2.15}$$

2.2.2 Constant adsorption

Adsorption and desorption models are commonly used to describe the concentration of VOCs and toxic substances in indoor environments. The simplest model considers a constant adsorption velocity v_d (see Table 2.2), which is proportional to the local concentration and the available surface area (Karlsson, 1994; Shair & Heitner, 1974; CPR 16E, 1989; Yuan, 2000), as shown in Eq. 2.16. This velocity has been found to be higher for reactive or water miscible gases than for non-reactive or immiscible gases (Jonsson *et al.*, 2005). Nevertheless, this velocity was also found to decrease with time and successive exposures (Karlsson, 1994). In the case of a toxic gas release, this velocity can be assumed to be constant. This is because the release does not last for a long time and the gas is not considered a common atmospheric pollutant, so the concept of successive exposures does not apply.

Table 2.2 Data on indoor adsorption velocities constants (Karlsson, 1994).

Gas	v_d (m·s^{-1})	Notes
NO_2	$1.4 \cdot 10^{-4}$	Residential rooms, air quality data $c_o/c_i = 2$, assumed *A/V = 2 m^{-1}*
	$1 \cdot 10^{-4} – 2 \cdot 10^{-4}$	Decrease rate measurements in residential rooms, assumed *A/V = 2 m^{-1}*
	$0.6 \cdot 10^{-4}$	Summary from literature on air quality
	$0.1 \cdot 10^{-4} – 8 \cdot 10^{-4}$	Decrease rate measurements in a box with a fan, various indoor materials.
O_3	$6 \cdot 10^{-4}$	Residential rooms, air quality data $c_o/c_i = 5$, assumed *A/V = 2 m^{-1}*
	$3.6 \cdot 10^{-4}$	Summary from literature on air quality
	$3 \cdot 10^{-3} – 5 \cdot 10^{-4}$	Decrease rate measurements in residential rooms, assumed *A/V = 2 m^{-1}*
Cl_2	$9 \cdot 10^{-5} – 1 \cdot 10^{-4}$	Decrease rate measurements in test rooms, fan to mix the air, initial concentration 15 ppm, *A/V = 2.1 m^{-1}*
SO_2	$1.4 \cdot 10^{-4}$	Residential rooms, air quality data $c_o/c_i = 2$, assumed *A/V = 2 m^{-1}*
NH_3	$3 \cdot 10^{-5} – 5 \cdot 10^{-5}$	Decrease rate measurements in test rooms, fan to mix the air, initial concentration 75 ppm, *A/V = 3.2 m^{-1}*
Trialkyl-phosphono-acetate (VX)	$2.6 \cdot 10^{-4} \pm 1.6 \cdot 10^{-4}$	Decrease rate measurements in test rooms, with surrogate of nerve agent VX, fan to mix the air. Release amount planned to give initial concentration in case of v_d=0 m·s^{-1}, A/V= 2.2–3.5 m^{-1}

$$R = v_d \cdot A \cdot C_i \qquad \text{Eq. 2.16}$$

In some situations, subsequent desorption (the re-emission of adsorbed substances) can occur, causing the remaining indoor concentration to be maintained for a long time after a release event (Karlsson & Huber, 1996; Zhang *et al*., 2002a). Desorption takes place when indoor concentration reaches values lower than equilibrium concentration (due to mixing with makeup air), causing the driving force (i.e. the concentration difference) to change the direction of the mass transfer. Three kinds of models for describing this behavior can be found in the literature: a one-sink model based on a simplification of Langmuir's theory (Bouhamra & Elkilani, 1999; Jørgensen & Bjørseth, 1999; Jørgensen *et al*., 1999; Karlsson & Huber, 1996; Won *et al*., 2001a; Won *et al*., 2001b), a sink-diffusion model (Jørgensen *et al*., 2000) and a two-sink model (Singer *et al*., 2004).

2.2.3 One-sink model based on a simplification of Langmuir's theory

Sink models are commonly based on general adsorption theory and may use a variety of adsorption isotherm models. The one-sink case refers to isotherms like Langmuir's isotherm that assume a monomolecular layer of adsorption sites with equal affinity to the adsorbed substance. This model gives a simple description of mass transport between the air and the adsorption surface. The relationship between the flux of gas deposited on the surface (dm_j/dt) and the indoor concentration is represented by Eq. 2.17, in which the losses and gains of Eq. 2.13 are combined in a single expression:

$$-\frac{R}{V}+\frac{S}{V}=-\sum_{j}^{D}\left(\frac{A_j}{V}\right)\cdot\frac{dm_j}{dt} \qquad \text{Eq. 2.17}$$

Some authors have developed different expressions for calculating gas flux (Jørgensen *et al.,* 2000; Karlsson & Huber, 1996). In fact, all of these expressions are equivalent, and the only thing that varies is the arrangement of the constants. Generally, it is assumed that the surface adsorption rate is proportional to the indoor concentration (C_i), while desorption is proportional to the amount of gas adsorbed on the surface m_j.

Thus, a mass balance for the material surface can be written as follows:

$$\frac{dm_j}{dt}=k_{a,j}\cdot C_i-k_{d,j}\cdot m_j, \quad j=1...D \qquad \text{Eq. 2.18}$$

Table 2.3 shows the values of k_a and k_d for some toxic substances. Values for VOCs can be found elsewhere (Bouhamra & Elkilani, 1999; Jørgensen & Bjørseth, 1999; Jørgensen *et al*., 1999; Jørgensen *et al*., 2000; Singer *et al*., 2004; Van Loy *et al*., 2001; Won *et al*., 2001a; Won *et al*., 2001b; Zhang *et al*., 2003).

This model has some drawbacks; for instance, it does not correctly model the behavior at high exposures and strong adsorptions (Van Loy *et al*., 1997), and it does not easily characterize the desorption curve tail for complex materials (e.g. fleecy materials such as carpets). The models described below, which were developed to represent more complex adsorption/desorption processes, take therefore into account diffusion into materials.

Table 2.3 Experimental values of k_a and k_d. Adapted from Karlsson and Huber (1996).

Agent	Material	k_a ($m \cdot s^{-1}$)	k_d (s^{-1})
Sarin	Glass silanized with Si (empty box)	$4.4 \cdot 10^{-5} \pm 0.83 \cdot 10^{-5}$	$9.7 \cdot 10^{-4} \pm 3.1 \cdot 10^{-4}$
	Plastic coated wallpaper on plasterboard	$1.7 \cdot 10^{-4} \pm 1.3 \cdot 10^{-4}$	$7.7 \cdot 10^{-5} \pm 7.5 \cdot 10^{-5}$
	Rouge spruce	$1.3 \cdot 10^{-4} \pm 2 \cdot 10^{-4}$	$9.5 \cdot 10^{-5} \pm 1.8 \cdot 10^{-4}$
	Unpainted concrete	$7.2 \cdot 10^{-4} \pm 3.1 \cdot 10^{-4}$	$1.9 * 10^{-5} \pm 1.4 \cdot 10^{-5}$
	Old chalking paint on concrete	$1.8 \cdot 10^{-4}$	$1.6 \cdot 10^{-6}$
	Glass	$4.3 \cdot 10^{-5}$	$1.7 \cdot 10^{-4}$
	Textile	$2.4 \cdot 10^{-4}$	$2.3 \cdot 10^{-5}$
	Wall hanging	$1.4 \cdot 10^{-4}$	$2.2 \cdot 10^{-5}$
VX Surrugate	Painted walls, roof and flat plastic carpet	$2.5 \cdot 10^{-4} \pm 1.2 \cdot 10^{-4}$	$1.8 \cdot 10^{-5} \pm 1.1 \cdot 10^{-5}$
NH_3	Painted walls, roof and flat plastic carpet	$1.1 \cdot 10^{-4} \pm 0.4 \cdot 10^{-4}$	$5.5 \cdot 10^{-6} \pm 2.3 \cdot 10^{-6}$
Cl_2	Painted walls, roof and flat plastic carpet	$1.4 \cdot 10^{-4} \pm 0.6 \cdot 10^{-4}$	$4.6 \cdot 10^{-6} \pm 2.6 \cdot 10^{-6}$
Acrolein (Singer *et al.*, 2004)	50 m^3 chamber with gypsum wallboard (with latex paint), floor carpet, wood-veneer furniture, pleated cotton drapery covering and four chairs with polyurethane foam cushioning (A/V=2.444 m^{-1})	$5.68 \cdot 10^{-6}$	$1.10 \cdot 10^{-5}$

2.2.4 Sink-diffusion model

This model considers two forms of mass transfer through three layers (Figure 2.3). From the first layer (the environment), the gas is adsorbed on the material surfaces in the room (1st sink) and then diffuses into the material (2nd sink). The entire process is considered reversible, and the bulk material is assumed to interact only with the surface. The flux of gas to and from the material surface is given as follows:

$$\frac{dm_{1,j}}{dt} = k_{a,j} \cdot C_i - k_{d,j} \cdot m_{1,j} - \frac{dm_{2,j}}{dt} \qquad j = 1...D \qquad \text{Eq. 2.19}$$

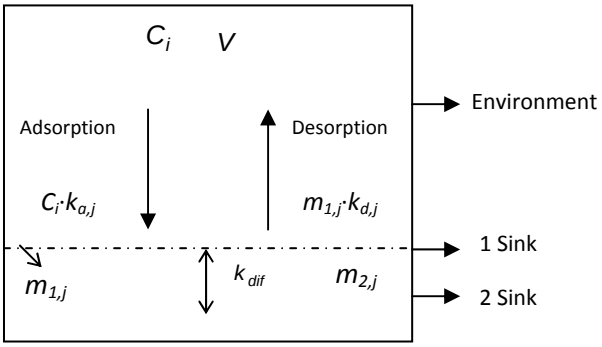

Figure 2.3 Representation of adsorption and desorption processes for a sink-diffusion model

It has been reported that the interaction between the surface and the bulk material can be described by Fick's Law using and equilibrium-interface model (Meininghaus & Uhde, 2002; Yang *et al*., 2001; Zhang *et al*., 2002a, 2002b; Zhao *et al*., 2002). Due to a lack of data on material properties and the complexity of the calculation, the interaction between the surface and the embedded sink is estimated by the one dimensional equation of Fick's law, using an effective mass transfer coefficient (Jørgensen *et al*., 2000; Singer *et al*., 2004):

$$\frac{dm_{2,j}}{dt} = k_{dif,j} \cdot \left(m_{1,j} - m_{2,j}\right) \qquad j = 1...D \qquad \text{Eq. 2.20}$$

The set of differential equations resulting from this model (Eq. 2.19 and Eq. 2.20) is better than Langmuir's model at predicting adsorption and desorption phenomena, especially in materials such as carpets or solid matrices.

2.2.5 Two-sink model

This model is similar to the previous one, but instead of k_{dif}, it uses two different mass transfer coefficients to represent the mass transfer between the surface and the bulk material (Figure 2.4). Physically, these unequal rates lead to a better representation of the mass transfer inside the material:

$$\frac{dm_{2,j}}{dt} = k_{1,j} \cdot m_{1,j} - k_{2,j} \cdot m_{2,j} \qquad j = 1...D \qquad \text{Eq. 2.21}$$

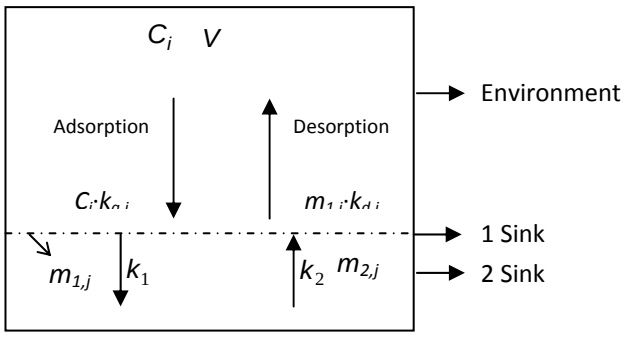

Figure 2.4 Representation of adsorption and desorption processes for a two-sink model

Table 2.4 shows some experimental values of k_a, k_d, k_{dif}, k_1 and k_2 for some surrogates of the related G-type nerve agents (highly toxic organophosphorus compounds), as measured by Singer *et al*. (2005a, 2005b). These measurements range from experimental chambers furnished with new or aged wallboard and plush or hard surfaces to residential bedrooms with different levels of furnishings. The parameters reported for residential rooms were the result of fit measurements from six residential experiments. Faster adsorption was reported for new wallboard than for aged wallboard, and plush surfaces were found to increase sorption rates. This behavior with regard to plush and hard surfaces has also been reported in studies of VOC sorption on indoor surfaces (Jørgensen *et al*., 1999; Piadé *et al*., 1999; Van Der Wal *et al*., 1998; Won *et al*., 2000, 2001a, 2001b; Zhang *et al*., 2002a, 2002b). In these studies, differences among compounds in sorption rates on the same surfaces were attributed to the vapor pressure of the compounds (high adsorption for low vapor pressure) and to polarity (polar compounds adsorb more easily). Table 2.5 summarizes the various models presented here, that are based on the general model (Eq. 2.13), without considering filtration.

Table 2.4 Mass transfer parameters for G-type nerve agents surrogates.

Substance	Model	$k_a \cdot A/V$, h^{-1} (s^{-1})	k_d, h^{-1} (s^{-1})	k_{dif}, h^{-1} (s^{-1})	k_1, h^{-1} (s^{-1})	k_2, h^{-1} (s^{-1})
Values obtained in a room with aged wallboard, plush and hard furnishings (A/V=2.5 m^{-1}) (Singer *et al.,* 2005a).						
DMMP[a]	One-sink	1.4 ($3.89 \cdot 10^{-4}$)	0.04 ($1.11 \cdot 10^{-5}$)			
	Sink-diffusion	1.5 ($4.17 \cdot 10^{-4}$)	0.08 ($2.22 \cdot 10^{-5}$)	0.05 ($1.39 \cdot 10^{-5}$)		
	Two-sink	2.1 ($5.83 \cdot 10^{-4}$)	0.40 ($1.11 \cdot 10^{-4}$)		0.20 ($5.65 \cdot 10^{-5}$)	0.03 ($8.33 \cdot 10^{-6}$)
DEEP[b]	One-sink	1.6 ($4.44 \cdot 10^{-4}$)	0.04 ($1.11 \cdot 10^{-5}$)			
	Sink-diffusion	1.7 ($4.72 \cdot 10^{-4}$)	0.08 ($2.22 \cdot 10^{-5}$)	0.05 ($1.39 \cdot 10^{-5}$)		
	Two-sink	2.4 ($6.67 \cdot 10^{-4}$)	0.39 ($1.08 \cdot 10^{-4}$)		0.21 ($5.83 \cdot 10^{-5}$)	0.03 ($8.33 \cdot 10^{-6}$)
TEP[c]	One-sink	1.8 ($5 \cdot 10^{-4}$)	0.04 (1.11·10-^{5})			
	Sink-diffusion	1.9 ($5.28 \cdot 10^{-4}$)	0.09 ($2.50 \cdot 10^{-5}$)	0.05 ($1.39 \cdot 10^{-5}$)		
	Two-sink	2.5 ($6.94 \cdot 10^{-4}$)	0.37 ($1.03 \cdot 10^{-4}$)		0.21 ($5.83 \cdot 10^{-5}$)	0.04 ($1.11 \cdot 10^{-5}$)
Values obtained in a room with new wallboard, hard surface furnishings (A/V=2 m^{-1}) (Singer *et al.,* 2005a).						
DMMP[a]	One-sink	1 ($2.78 \cdot 10^{-4}$)	0.01 ($2.78 \cdot 10^{-6}$)			
	Sink-diffusion	1 ($2.78 \cdot 10^{-4}$)	0.02 ($5.56 \cdot 10^{-6}$)	0.04 ($1.11 \cdot 10^{-5}$)		
	Two-sink	2.2 ($6.11 \cdot 10^{-4}$)	0.72 ($2 \cdot 10^{-4}$)		0.19 ($5.28 \cdot 10^{-5}$)	0.01 ($2.78 \cdot 10^{-6}$)
DEEP[b]	One-sink	1.8 ($5 \cdot 10^{-4}$)	0.05 ($1.39 \cdot 10^{-5}$)			
	Sink-diffusion	1.9 ($5.28 \cdot 10^{-4}$)	0.10 ($2.78 \cdot 10^{-5}$)	0.05 ($1.39 \cdot 10^{-5}$)		
	Two-sink	2.9 ($8.06 \cdot 10^{-4}$)	0.53 ($1.47 \cdot 10^{-4}$)		0.13 ($3.61 \cdot 10^{-5}$)	0.02 ($5.56 \cdot 10^{-6}$)
TEP[c]	One-sink	2.1 ($5.83 \cdot 10^{-4}$)	0.06 ($1.67 \cdot 10^{-5}$)			
	Sink-diffusion	2.3 ($6.39 \cdot 10^{-4}$)	0.13 ($3.61 \cdot 10^{-5}$)	0.05 ($1.39 \cdot 10^{-5}$)		
	Two-sink	3.2 ($8.89 \cdot 10^{-4}$)	0.46 ($1.28 \cdot 10^{-4}$)		0.12 ($3.33 \cdot 10^{-5}$)	0.02 ($5.56 \cdot 10^{-6}$)
MS[d]	One-sink	2.4 ($6.67 \cdot 10^{-4}$)	0.09 ($2.5 \cdot 10^{-5}$)			
	Sink-diffusion	2.7 ($7.50 \cdot 10^{-4}$)	0.20 ($5.56 \cdot 10^{-5}$)	0.06 ($1.67 \cdot 10^{-5}$)		
	Two-sink	3.9 ($1.08 \cdot 10^{-4}$)	0.63 ($1.75 \cdot 10^{-4}$)		0.14 ($3.89 \cdot 10^{-5}$)	0.04 ($1.11 \cdot 10^{-5}$)
Values obtained in a residential room (A/V=4.56 m^{-1}) (Singer *et al.,* 2005b).						
DMMP[a]	One-sink	3.2 ± 1.4 ($8.89 \cdot 10^{-4}$ ± $3.89 \cdot 10^{-4}$)	0.09 ± 0.03 ($2.5 \cdot 10^{-5}$ ± $2.5 \cdot 10^{-5}$)			
	Sink-diffusion	3.5 ± 1.5 ($9.72 \cdot 10^{-4}$ ± $4.17 \cdot 10^{-4}$)	0.17 ± 0.06 ($4.72 \cdot 10^{-5}$± $1.67 \cdot 10^{-5}$)	0.21 ± 0.01 ($5.83 \cdot 10^{-5}$ ± $2.78 \cdot 10^{-6}$)		
	Two-sink	5.0 ± 1.5 ($1.39 \cdot 10^{-3}$ ± $4.17 \cdot 10^{-4}$)	0.86 ± 0.40 ($2.39 \cdot 10^{-4}$± $1.11 \cdot 10^{-4}$)		0.72 ± 0.16 ($2 \cdot 10^{-4}$ ± $4.44 \cdot 10^{-5}$)	0.12 ± 0.04 ($3.33 \cdot 10^{-5}$ ± $1.11 \cdot 10^{-5}$)
DEEP[b]	One-sink	3.3 ± 1.3 ($9.17 \cdot 10^{-4}$ ± $3.61 \cdot 10^{-4}$)	0.12 ± 0.03 ($3.33 \cdot 10^{-5}$± $8.33 \cdot 10^{-6}$)			

[a] DMMP (dimethyl methylphosphonate), surrogate for sarin (GB).
[b] DEEP (diethyl ethylphosphonate), surrogate for soman (GD).
[c] TEP (triethyl phosphate), surrogate for tabun (GA).
[d] MS (methyl salicylate), surrogate of mustard gas.

Table 2.5 Models derived to estimate indoor concentration based on Eq. 2.15.

Model	Final expression	
No adsorption	$\frac{dC_i}{dt} = ACH \cdot (C_o - C_i)$	Eq. 2.22
Constant adsorption model	$\frac{dC_i}{dt} = ACH \cdot C_o - ACH \cdot C_i - v_d \cdot \frac{A}{V} \cdot C_i$	Eq. 2.23
One-sink model	$\frac{dC_i}{dt} = ACH \cdot C_o - ACH \cdot C_i - \sum_j^D \left(\left(\frac{A_j}{V} \right) \cdot \left(k_{a,j} \cdot C_i - k_{d,j} \cdot m_j \right) \right)$	Eq. 2.24
Sink-diffusion model	$\frac{dC_i}{dt} = ACH \cdot C_o - ACH \cdot C_i - \sum_j^D \left(\left(\frac{A_j}{V} \right) \cdot \left(k_{a,j} \cdot C_i - k_{d,j} \cdot m_{1,j} - k_{dif,j} \cdot \left(m_{1,j} - m_{2,j} \right) \right) \right)$	Eq. 2.25
Two-sink model	$\frac{dC_i}{dt} = ACH \cdot C_o - ACH \cdot C_i - \sum_j^D \left(\left(\frac{A_j}{V} \right) \cdot \left(k_{a,j} \cdot C_i - k_{d,j} \cdot m_{1,j} - k_{1,j} \cdot m_{1,j} + k_{2,j} \cdot m_{2,j} \right) \right)$	Eq. 2.26

2.3 Outdoor concentration

To predict the evolution of a toxic cloud caused by an accidental release as a function of position and time, one of the most important parameters is the duration of the release. When an accidental release takes place, the emission can be classified as either continuous or instantaneous. This classification is not as simple as it seems. It is usually made according to the duration of the release and the location (downwind distance from the source) at which the concentration is measured (Casal, 2008). For example, a continuous emission takes place if the duration of the release is longer than the time required for the cloud to reach a given location, while an instantaneous emission is considered if the time required to reach a given location is longer than the duration of the emission. The distinction between continuous and instantaneous can be evaluated quantitatively using Eq. 2.27 (Casal *et al.*, 1999a). Nevertheless, it should be clarified that a continuous release does not necessarily mean a continuous source.

Continuous: $x > 1.8 \cdot v \cdot t_1$

Instantaneous: $x \leq 1.8 \cdot v \cdot t_1$ Eq. 2.27

Gaussian dispersion models are often used to describe the atmospheric dispersion of gases whose density is similar to that of air (i.e. neutral gases), as well as heavier-than-air gases that are sufficiently diluted at the source. In the case of heavy gases, the simulation is more complex and the dispersion must be computed solving a set of differential equations numerically. These equations correlate the slow down and spread of the dense cloud, the entrance of air, the heat transfer with the ground and the mass, momentum and heat transfer. Examples of these models are the DEGADIS and SLAB (Carrari *et al*., 2004; Dandrieux *et al*., 2006; Casal *et al*., 1999a), which are numeric codes available in different commercial programs like ALOHA or BREEZE HAZ. Since heavy gases are more complex, and the calculation of outdoor dispersion is not the aim of the present thesis, only the Gaussian model is described.

The Gaussian model is based on the following simplifying assumptions:

- The mass flow rate is assumed to be constant throughout the emission.
- All of the mass emitted from the source remains in the atmosphere (i.e. no chemical reactions take place).
- There are no gravitational effects on the emitted material.
- The meteorological conditions are constant over time.
- The ground roughness is uniform in the dispersion area.

Eq. 2.28 and Eq. 2.29 correspond to Gaussian dispersion models for continuous and instantaneous sources, respectively (Casal, 2008).

$$C_o(x,y,z) = \frac{\dot{q}}{2 \cdot \pi \cdot v \cdot \sigma_y \cdot \sigma_z} \cdot \exp\left(-\frac{y^2}{2 \cdot \sigma_y^2}\right) \cdot \left[\exp\left(-\frac{(z-h)^2}{2\sigma_z^2}\right) + \exp\left(-\frac{(z+h)^2}{2\sigma_z^2}\right)\right] \quad \text{Eq. 2.28}$$

$$C_o(x,y,z,t') = \frac{q}{(2\pi)^{3/2} \cdot \sigma_{x,i} \cdot \sigma_{y,i} \cdot \sigma_{z,i}} \cdot \exp\left(-\frac{(x - v \cdot t')^2}{2\sigma_{x,i}^2} - \frac{y^2}{2\sigma_{y,i}^2}\right) \cdot \left[\exp\left(-\frac{(z-h)^2}{2\sigma_{z,i}^2}\right) + \exp\left(-\frac{(z+h)^2}{2\sigma_{z,i}^2}\right)\right] \quad \text{Eq. 2.29}$$

Accidental releases commonly last for a short period of time (typically less than 60 min). Therefore, to represent the concentration during the cloud passage, two approaches could be employed, to use a block function or a set of equations. The block function, known as a temporary source (CPR 16E, 1989), represents a time-limited release where a steady state concentration is reached for a particular period of time. The block function is expressed as:

$$\begin{aligned} C_o &= 0 \quad \text{for} \quad t < 0 \\ C_o &= C_o(x) \quad \text{for} \quad 0 \le t \le t_1 \\ C_o &= 0 \quad \text{for} \quad t > t_1 \end{aligned} \qquad \text{Eq. 2.30}$$

Where $C_o(x)$ is the outdoor concentration corresponding to the Gaussian continuous source (Eq. 2.28), and t = 0 denotes the time when the plume arrives at point x. Therefore, there is no connection with the time the release started, and so, this approach is useful for single point calculations, and when the time elapsed from the beginning of the release is not necessary.

The second approach consists of using the Gaussian equations presented by Seinfeld & Pandis (1998). These equations allow the estimation of the outdoor concentration as a function of time from the start of the release (*t'*), even in the case of an instantaneous release. They consist of two equations, one to perform the calculation before the emission finishes (Eq. 2.31) and another after it finishes (Eq. 2.32). The term $C_o(x,y,z)$ correspond to the concentration for a continuous source given by Eq. 2.28.

$$C_o(x,y,z,t') = \frac{1}{2} C_o(x,y,z) \left[erf\left(\frac{x}{\sigma_x \sqrt{2}} \right) - erf\left(\frac{x - vt'}{\sigma_x \sqrt{2}} \right) \right] \qquad t' \le t_1 \qquad \text{Eq. 2.31}$$

$$C_o(x,y,z,t') = \frac{1}{2} C_o(x,y,z) \left[erf\left(\frac{x - v(t' - t_1)}{\sigma_x \sqrt{2}} \right) - erf\left(\frac{x - vt'}{\sigma_x \sqrt{2}} \right) \right] \qquad t' > t_1 \qquad \text{Eq. 2.32}$$

The standard deviations used in these expressions are calculated from Eq. 2.33 to Eq. 2.35, using the parameters of Table 2.6 depending on the atmospheric stability class and the terrain surface roughness.

$$\sigma_x = \left[{\sigma_y}^2 + 0.09\left(\frac{h + 0.5\sigma_z}{h + 0.17\sigma_z} \right)^{2p} \left(\frac{p \cdot x}{h + 0.5\sigma_z} \right)^2 {\sigma_z}^2 \right]^{0.5} \quad \text{Eq. 2.33}$$

$$\sigma_y = \exp\left(I_y + J_y \ln x + K_y (\ln x)^2 \right) \quad \text{Eq. 2.34}$$

$$\sigma_z = \exp\left(I_z + J_z \ln x + K_z (\ln x)^2 \right) \quad \text{Eq. 2.35}$$

Table 2.6 Parameters for the calculation of dispersion coefficients (Irwin, 1979)

Parameter		Atmospheric Stability					
		Very Unstable (A)	**Unstable (B)**	**Slightly Unstable (C)**	**Neutral (D)**	**Slightly Stable (E)**	**Stable (F)**
I_y		-1.1040	-1.6340	-2.054	-2.555	-2.754	-3.143
J_y		0.9878	1.0350	1.0231	1.0423	1.0106	1.0148
K_y		-0.0076	-0.0096	-0.0076	-0.0087	-0.0064	-0.0070
I_z		4.6790	-1.9990	-2.341	-3.186	-3.783	-4.490
J_z		-1.7172	0.8752	0.9477	1.1737	1.3010	1.4024
K_z		0.2770	0.0136	-0.0020	-0.0316	-0.0450	-0.0540
p	z_o=0.01m	0.05	0.06	0.06	0.12	0.34	0.53
	z_o=0.1m	0.08	0.09	0.11	0.16	0.32	0.54
	z_o=1m	0.17	0.17	0.20	0.27	0.38	0.61
	z_o=3m	0.27	0.28	0.31	0.37	0.47	0.69

2.3.1 Expressions for C_i in the cases of no adsorption and constant adsorption

Explicit equations for the estimation of C_i, when outdoor dispersion is simulated using the Gaussian model, have been reported (CPR 16E, 1989; Casal *et al*., 1999b, 2008) for the cases with no adsorption (Eq. 2.22) and for constant adsorption (Eq. 2.23). The solution of Eq. 2.23 with the limiting conditions C_i = 0 as t = 0 is given as follows:

$$C_i(t) = ACH \cdot \int_0^t C_o(t') \exp(-\dot{n}_{oa}(t - t'))dt' \quad \text{Eq. 2.36}$$

where $\dot{n}_{oa} = ACH + \frac{v_d \cdot A}{V}$.

Table 2.7 shows analytical solutions to Eq. 2.36 for outdoor concentration represented by the three types of sources (Casal, 2008; CPR 16E, 1989). In the case of no adsorption, $v_d = 0$ and consequently $\dot{n}_{oa} = ACH$.

Table 2.7 Indoor concentration solutions applying the deposition model (Casal, 2008; CPR 16E, 1989).

Source	Expression		Conditions
Continuous	*Ci(t)*=0		t <0
	$C_i(t) = \frac{ACH}{\dot{n}_{oa}} C_o \left(1 - \exp\left(-\dot{n}_{oa} \cdot t\right)\right)^a$	Eq. 2.37	$t \geq 0$
Temporary	*Ci(t)*=0		t <0
	$C_i(t) = \frac{ACH}{\dot{n}_{oa}} C_o \left(1 - \exp\left(-\dot{n}_{oa} \cdot t\right)\right)^a$	Eq. 2.37	$0 \leq t \leq t_1$
	$C_i(t) = \frac{ACH}{\dot{n}_{oa}} C_o \left(\exp\left(\dot{n}_{oa} \cdot t_1\right) - 1\right) \exp\left(-\dot{n}_{oa} \cdot t\right)^a$	Eq. 2.38	$t > t_1$
Instantaneous	$C_i(t') = \frac{q \cdot ACH}{4 \cdot \pi \cdot v \cdot \sigma_{y,i} \cdot \sigma_{z,i}} \exp\left(-\frac{y^2}{2\sigma_{y,i}^2}\right) \left[\exp\left(-\frac{(z-h)^2}{2\sigma_{z,i}^2}\right) + \exp\left(-\frac{(z+h)^2}{2\sigma_{z,i}^2}\right)\right]$ $\exp\left(\frac{1}{2}\left(K^2 - \frac{x^2}{\sigma_{x,i}^2}\right)\right) \exp\left(-\dot{n}_{oa} \cdot t'\right) \left[erf\left(\frac{v \cdot t'}{\sigma_{x,i}\sqrt{2}} - \frac{K}{\sqrt{2}}\right) + erf\left(\frac{K}{\sqrt{2}}\right)\right]$		
	$K = \left(\sigma_{x,i}^2 \cdot \dot{n}_{oa} + v \cdot x\right) \Big/ \left(v \cdot \sigma_{x,i}\right)$	Eq. 2.39	

[a] C_o refers to the outdoor concentration at a distance x from the source, given by Eq. 2.28.

2.4 Estimation of the air exchange rate

Air infiltration refers to the flow of outdoor air through various leakage sites in a building (i.e. cracks and pores of the building shell, bad sealing between windows or door frames and walls, etc.), due to an indoor-outdoor pressure difference, mostly generated by meteorological conditions (wind and indoor-outdoor temperature difference). In order to estimate the air infiltration flow or the *ACH*, it is necessary to calculate the indoor/outdoor pressure difference and to know the characteristics of the leakage sites, either one by one or as a whole (i.e. envelope airtightness). Then, depending on the building's internal resistance to airflow (i.e. number of internal partitions or compartments), a multizone or single-zone model can be used

(ASHRAE, 2005). With small buildings such as single-family residences, which lack the complexity of multifamily residences or multi-story office buildings, the indoor air is often assumed to be homogeneously distributed. As a result, the whole house is considered as a single zone (Orme & Leksmono, 2002; Sherman & Grimsrud, 1980). On the other hand, large buildings (e.g. multi-family residences or multi-story office buildings) usually have high internal resistance to airflow (non-homogeneous distribution) and must therefore be modeled differently. Multizone models (i.e. a series of interconnected zones, with the assumption that the air within each zone is well-mixed) or computational fluid dynamics (CFD) models can be used in such cases. In addition to the mass and energy balances also used in multizone models, CFD models take into account the momentum effect. As a result, their predictions have been reported to be more accurate (Chen, 2009; Wang & Chen, 2008). However, due to the high complexity and computing time of these models (hours or even days) their applications are limited. In the case of single-family residences (e.g. the houses close to a toxic release location), the greater precision of the results does not make up for the complexity of these models (Emmerich, 2001). The analysis of multizone and CFD models is thus beyond of the scope of this study.

The *ACH* in single-family dwellings is usually determined empirically or semi-empirically. Empirical values are obtained using a tracer gas dilution technique, as described in the ASTM standard E741-00, however it should be noted that the results are specific to the prevailing meteorological conditions during the test period. In contrast, the semi-empirical method provides estimated values of *ACH* under different meteorological conditions. This approach consists of determining the envelope airtightness, using the pressurization technique (EN 13829: 2001), and then applying a ventilation model to estimate the infiltration airflow as a function of the meteorological conditions. Single-zone models such as the LBL model (Sherman & Grimsrud, 1980) or the AIM-2 model (Walker & Wilson, 1998) can be used to estimate the *ACH* as a function of the airtightness, the indoor-outdoor temperature difference and the wind speed.

2.4.1 Envelope Airtightness

The envelope airtightness of residential dwellings is usually measured with a pressurization technique (EN 13829:2001), which consists in pressurizing the house envelope with a large fan

or blower fitted in a door or a window and measuring the airflow required to maintain a certain indoor-outdoor pressure difference. Buildings with a higher degree of leakage require more airflow to maintain the pressure difference. Several pressure differences and airflow measurements are taken, and the dataset is then regressed to fit the power law equation (Eq. 2.40) and determine the power law coefficient (*c*) and power law exponent (*N*).

$$Q_{\Delta P} = c \cdot (\Delta P)^N \qquad \text{Eq. 2.40}$$

The exponent *N* can take a value in the range of 0.5-1 depending on the airflow pattern, which is characterized as laminar (close to 1) or turbulent (close to 0.5) (ASHRAE, 2005). For residential buildings this coefficient is usually in the range 0.6-0.7, and a typical value is 2/3 (Sherman, 1992). These power law constants can be used in single-zone infiltration models like the AIM-2 model to estimate the infiltration airflow as a function of wind speed and indoor-outdoor temperature difference.

Several indexes have been proposed to characterize the building airtightness. The objective of these indexes is to normalize the infiltration flow, at a certain pressure difference, in order to better compare the performance among buildings independently of the buildings characteristics. Most common indexes are the air exchange rate, $ACH_{\Delta P}$ (Eq. 2.41), which uses the indoor heated volume as the normalization parameter; the leakage index, $I_{\Delta P}$ (Eq. 2.42), which uses the envelope unheated surface area (S_f) (the surface that separates the indoor heated volume from the outdoor air and unheated spaces) as the normalization parameter (Litvak *et al*., 2000a); and the normalized leakage area, *NL* (Eq. 2.43), in which the airflow is converted to an equivalent leakage area (*ELA*) and is then normalized by the floor area(Area) and height (*H*). The *ELA* is obtained based on Bernoulli's equation of the flow through an orifice, and therefore, it represents the area of an opening (with an assumed value of C_D) that if exposed to the same pressure difference as the dwelling, would lead to the same leakage airflow as shown in Eq. 2.44. The pressure difference, at which the *NL* is defined in ASHRAE (2005), is 4 Pa.

$$ACH_{\Delta P} = Q_{\Delta P} / V \qquad \text{Eq. 2.41}$$

$$I_{\Delta P} = Q_{\Delta P} / S_f \qquad \text{Eq. 2.42}$$

$$NL = 1000\left(\frac{ELA}{Area}\right)\left(\frac{H}{H_o}\right)^{0.3} \quad \text{Eq. 2.43}$$

$$ELA = Q \cdot \frac{\sqrt{\rho/2 \cdot \Delta P}}{C_D} = \frac{c}{C_D}\left(\Delta P_r\right)^{N-0.5}\sqrt{\frac{\rho}{2}} \quad \text{Eq. 2.44}$$

For the characterization of the airtightness distribution of single-family dwellings, Orme *et al*. (1998) have proposed a series of worksheets for estimating the value of ACH_{50} depending on the building type, the construction techniques and the height of the building (low-rise or high-rise building), based on the Air Infiltration and Ventilation Centre (AIVC) database. Most recent efforts on this field are those made by the Lawrence Berkeley National Laboratory (LBNL), which developed a predictive model to estimate the *NL* of US single-family dwellings, as a function of buildings characteristics, using the LBNL air leakage database.

LBNL airtightness predictive model

The LBNL airtightness predictive model (Eq. 2.45), developed by McWilliams and Jung (2006), estimates the value of *NL* as a function of climatic zone (*CZ*), floor area (*size*), height (N_{story}), age (*Age*), possibility of floor leakage (P_{floor}), possibility of participation in an energy efficiency program (P_{Eff}), and possibility of being a low-income house (P_{LI}). The variable *size* in the model refers to the ratio between the floor area and a reference area of 100 m^2. The *P* parameters (P_{LI}, P_{Floor} and P_{Eff}) reflect the possibility that the house meets the given condition, taking a value of 1 if the condition is met and a value of 0 if it is not. The energy efficient parameter describes the impact that energy efficiency programs have on building airtightness. For this variable authors found a significant difference between the airtightness of dwellings that had participated on these programs (among 40% tighter) and those that had not. The low income parameter represents low income houses which were found to be almost two times leakier than references dwellings. The floor leakage parameter represents the difference between the airtightness of houses that are slab-on-grade, which are generally tight than dwellings with vented crawl-spaces.

The values for the climatic zones and the variables coefficients are shown in Table 2.8, where the NL_{CZ} parameter depends on the climatic zone in which the house is located. McWilliams and Jung (2006) consider four climatic zones "humid", "cold", "dry" and "Alaska", based on combinations of the climatic zones defined by the Building Science Corporation, which

classifies zones according to annual precipitation and heating degree days (Building Science Consulting, 2007), as shown in Table 2.9. Although this model is inaccurate for individual predictions, it has been reported to give reasonable estimations of leakage distributions when applied to populations of houses (Sherman, 2008).

$$NL = NL_{CZ} \cdot \phi_{area}^{size-1} \cdot \phi_{height}^{N_{story}-1} \cdot \phi_{\varepsilon}^{P_{eff}} \cdot \phi_{age}^{age} \cdot \phi_{floor}^{P_{floor}} \cdot \left(\phi_{LI,age}^{age} \cdot \phi_{LI,area}^{size-1} \cdot \phi_{LI}\right)^{P_{LI}} \quad \text{Eq. 2.45}$$

Table 2.8 Parameters in the LBNL predictive model (McWilliams & Jung, 2006)

***NL*cz**	**Value**	**Parameter**	**Value**	**Parameter**	**Value**
NL_{Alaska}	0.36	ϕ_{height}	1.156	ϕ_{Floor}	1.08
NL_{Cold}	0.53	ϕ_{ε}	0.598	ϕ_{LI}	2.45
NL_{Humid}	0.35	ϕ_{Age}	1.0118	$\phi_{LI,Age}$	0.9942
NL_{Dry}	0.61	ϕ_{Area}	0.841	$\phi_{LI,Area}$	0.775

Table 2.9 Definition of climate zones used in the LBNL model.

Dry	Consists of Marine, Hot-Dry and Mixed-Dry zones. It refers to a region that receives less than 500 mm of annual precipitation, and has approximately 5400 heating degree days (HDD) or less. The HDD is a quantitative index designed to reflect the demand for energy needed to heat a home, they are defined relative to a base temperature (18ºC), and accounts for the difference between the base temperature and the average outside temperature during the day (when it is lower than the base temperature), the sum of these difference across the year gives the total HDD.
Humid	Consists of Hot-Humid and Mixed-Humid zones. Is defined as a region that receives more than 500mm of annual precipitation and has approximately 5400 HDD or less.
Cold	Consist of Cold and Very Cold regions. This climate is defined as a zone with approximately 5400 HDD or greater and less than approximately 12600
Alaska	A zone defined by the model developers that include all the data from this state.

2.4.2 Single-zone ventilation models

These models are considered as the simplest ventilations models, since they treat the building as a single zone, where indoor air is assumed to be homogeneously distributed. The advantage of these models is that they can be easily configured; they use a minimum of data (do not need individual component airtightness, size and location of designed ventilation provisions, or wind pressure coefficient) and are quick. However, the speed and simplicity is at the expenses of

accuracy and detailed results, like airflow patterns inside the zone. These models use the whole airtightness of the building and combine it with meteorological conditions to predict the airflow (Orme & Leksmono, 2002). Most common single-zone models used comprise the LBL model (Sherman & Grimsrud, 1980) which uses the *ELA*, and the AIM-2 model (Walker & Wilson, 1998), which uses *c* and *N* of the power law equation (Eq. 2.40). The AIM-2 model differs from other single-zone models described in the literature in the following ways: it uses the power law to represent the envelope leakage; it distinguishes between dwellings with crawl spaces or slab-on-grade foundations; and it considers the furnace flue as a separate leakage site. As a result of these differences, the AIM-2 has been reported (Walker & Wilson, 1998; Wang *et al*., 2009), to give more accurate predictions of ventilation rates under different conditions (i.e. houses with and without furnace flues, wind or stack dominated ventilation), and to have an overall predictive accuracy in the order of ±10% (ASHRAE, 2005). In the study done by Walker and Wilson (1998), they found that the model tends to overestimate the *ACH* by about 8% for unsheltered dwellings and wind-dominated conditions while it may underestimate infiltration by about 10% for sheltered dwellings at either stack- or wind-dominated conditions. Moreover, in the work developed by Wang *et al*. (2009) they reported a tendency of the model to underestimate the *ACH* by about 5%.

AIM-2 Model

The AIM-2 model estimates the infiltration flow (Q) as a combination of the flows induced by the wind effect (Q_w), represented by the wind speed, and the stack effect (Q_s), which reflects the indoor-outdoor temperature difference; the value of these flows depends, in turn, on the flow coefficient (c_1), the pressure difference generated by each effect, and the coefficient factors of each effect. The wind factor (f_w) depends on the presence or absence of a flue and the possibility of slab-on-grade or crawl space foundation. The total shelter factor (S_w) gives an estimation of the overall shelter provided by the surroundings of the dwelling; it combines the building shelter situation and the flue shelter depending on adjacent obstacles (Table 2.10). The stack factor (f_s) is influenced by the presence of a flue and the height of the dwelling, represented by the number of stories.

The main equations of the AIM-2 model are:

$$Q = \left(Q_s^{1/N} + Q_w^{1/N} + B_1 \cdot (Q_s \cdot Q_w)^{1/2N}\right)^N \quad \text{Eq. 2.46}$$

$$Q_s = c_1 \cdot f_s \cdot \Delta P_s^N \quad \text{Eq. 2.47}$$

$$\Delta P_s = \rho \cdot g \cdot H \cdot \left(|T_i - T_o| / T_i\right) \quad \text{Eq. 2.48}$$

$$Q_w = c_1 \cdot f_w \cdot \Delta P_w^N \quad \text{Eq. 2.49}$$

$$\Delta P_w = \rho \cdot (S_w \cdot v)^2 / 2 \quad \text{Eq. 2.50}$$

$$c_1 = c + c_{flue} \quad \text{Eq. 2.51}$$

$$Y = c_{flue} / c_1 \quad \text{Eq. 2.52}$$

A detailed description of estimating the stack, wind and wind shelter factors can be found in Walker and Wilson (1998).

Table 2.10 Estimates of shelter coefficient (Walker & Wilson, 1998)

Terrain description	Shelter coefficient S_w
No obstructions or local shielding	1
Light local shielding with few obstructions within two buildings	0.9
Local shielding with many large obstructions within two building heights	0.7
Heavily shielded, many large obstructions within one building height	0.5
Complete shielding with large buildings immediately adjacent	0.3

The wind related data is an important consideration when modeling ventilation. Usually wind speed is available from measurements made at meteorological stations which are located at a significant distance from the site of interest and under other terrain conditions (i.e. open sites). Therefore a conversion must be made from these velocities measured at a reference height and terrain to velocities at the building location at building's height and terrain conditions. One of the conversions most used is the one adopted in the LBL model (Orme & Leksmono, 2002), and described in Eq. 2.53.

$$v_z = v_{z'} \frac{\delta(z/10)^{\gamma}}{\delta'(z'/10)^{\gamma'}}$$ Eq. 2.53

Where v_z is the required site wind speed at level z above ground, v' is the measured wind speed at level z' above ground, δ' and γ' are constants dependent on offsite terrain conditions, and δ and γ are constants dependent on onsite terrain conditions (Table 2.11).

Table 2.11 Onsite and offsite terrain-dependent constants used in the LBL model (Orme & Leksmono, 2002)

Terrain description	γ or γ'	δ or δ'
Ocean or other body of water with at least 5 km of unrestricted expanse.	0.10	1.30
Flat terrain with some isolated obstacles, e.g. buildings or trees well-separated from each other	0.15	1.00
Rural areas with low buildings, trees, etc.	0.20	0.85
Urban, industrial or forest areas.	0.25	0.67
Centre of large city.	0.35	0.47

2.4.3 Experimental data and behavior of the airtightness

Air infiltration in single-family dwellings has become a popular research area over the last three decades, because it greatly influences the energy performance of buildings and indoor air quality. For these reasons, several experimental campaigns have been carried out in different countries with the aim of quantifying the energy performance of residences in terms of envelope airtightness and existing directives, in order to improve the thermal regulations for new buildings.

Airtightness in residential buildings

Current studies focus on qualitative and quantitative analysis of available airtightness and *ACH* measurements to determine distributions and trends. Sherman and Dickerhoff (1998), for example, analyzed the single-family dwellings airtightness dataset compiled by the LBNL in order to determine the influence that basement type, age, presence of a duct system, number of stories and participation in weatherization assistance programs have on the normalized leakage area (*NL*). These authors found that dwellings with crawlspace or unconditioned basement were leakier than those with conditioned basements or slab-on-grade; that newer

dwellings were tighter than older; and that multistory dwellings were also leakier than one story. Concerning the dwellings that participate in a weatherization program, the authors reported a reduction of 25% in the *NL* after the weatherization. Orme *et al*., (1998) analyzed the AIVC database, which contains airtightness data for buildings in different countries. They examined the behavior of *ACH* at 50 Pa over a wide range of dwellings with different occupancy modes, years of construction and construction techniques. They concluded that multifamily dwellings are more airtight than single-family dwellings, that construction type and year of construction have a strong influence on airtightness (new constructions are more airtight), and that dwellings located in severe climate regions are more airtight. Table 2.12 show the mean and standard deviation of the *ACH* for residences in different countries found by these authors. As a result of their analysis they also proposed a series of worksheets to make an initial guess of the *ACH* at 50 Pa based on construction techniques.

Table 2.12 Mean *ACH* for residences in different countries (Orme *et al*., 1998)

Country	Sample size	ACH_{50} (h^{-1})	
		Mean	Standard deviation
Belgum	57	8.23	7.22
Canada	474	5.31	3.28
France	66	3.59	2.03
Netherlands	303	10.14	6.71
New Zealand	83	9.48	4.86
Norway	40	4.95	1.83
Sweden	144	5.10	3.81
Switzerland	37	3.22	1.48
UK	385	13.62	5.71
US	435	11.18	6.23

Statistical analysis of air leakage datasets for single-family dwellings has also been performed recently by the LBNL (Chan *et al*., 2005; McWilliams & Jung, 2006). These analyses deal with the development of predictive models for estimating the *NL* of single-family dwellings in the US as a function of dwelling characteristics. The model developed by Chan *et al*. (2005) takes into account the year of construction and the floor area as predictor variables, for three types of dwellings: low-income dwellings, energy program dwellings and conventional dwellings. The model developed later by McWilliams and Jung (2006) is based on a larger dataset and

predicts the value of *NL* as a function of climatic zone, building age, floor area, building height, floor type, energy-efficiency and low-income classifications as explained in section 2.4.1.

Concerning the southwest of Europe France is the leading nation in this research field. French researchers have typically focused on determining the main air leakage paths and exploring airtightness patterns for different construction types (masonry or timber frame), occupancy modes (single or multifamily dwellings) and insulation types (interior, integrated and exterior thermal insulation), using the pressurization technique (Litvak *et al*., 2000a, 2000b; Carrié *et al*., 2006). From their work, they concluded that multifamily dwellings (ACH_{10} = 0.5 h^{-1}) were more airtight than single-family dwellings (ACH_{10} = 1.1 h^{-1}), that masonry buildings (ACH_{10} = 0.7 h^{-1}) were more airtight than those with timber frames (ACH_{10} = 1.4 h^{-1}), and that no trends were observed for thermal insulation types. They also found that the leakiest parts of the building envelope were the indoor chests of shutters, the bonding between window frames and walls, the electric outlets and the bonding between floors and walls. Table 2.13 shows the reference and default values of the airtightness stipulated by the French thermal regulation to estimate the energy performance of new buildings (Carrié *et al*., 2006). The reference value could be used if constructions materials met some requirements; if not, the default value might be used.

Table 2.13 Reference and default airtightness values in the French thermal regulation (Carrié *et al.*, 2006)

Usage	Reference, I_4	Default, I_4
Single-family dwellings	0.8	1.3
Other residential buildings, offices, restaurants, educational and sanitary buildings	1.2	1.7
Other usages	2.5	3.0

Airtightness in public and commercial buildings

An extensive study on this type of buildings is the one done by Persily (1999), which includes 139 measurements of office buildings, schools, industries and others; from different countries (United States, Canada, Sweden and England). In this work, the author uses the I_{75} as the airtightness indicator, and compares the results in terms of height, year of construction, type of construction, building age and type of building. The buildings' distribution and the mean I_{75} by building type are shown in Table 2.14, where it can be seen that industrial buildings in

Sweden and colleges in New York are the tightest, while Florida's industrial buildings and Canada's commercial buildings are the leakiest.

Table 2.14 Airtightness data in public and commercial buildings (Persily, 1999)

Building type	Country/ State	Sample size	Mean number of stories	Mean age (years)	Range of age	I_{75}	
						Mean	Standard deviation
NIST Offices	US	8	6.1	18.3	8 – 23	15.3	12.3
NRC Offices	Canadá	8	18.5	27.5	24 – 34	10.6	5.4
BRE Offices	UK	10	NA*	17.2	7 – 35	23.3	11.9
Flo. Offices	US/ Florida	22	1	25.8	4 – 67	36.0	28.6
N.Y. Schools	US/ N.Y.	13	NA	NA	NA	8.5	4.3
NRC. Schools	Canada	11	1	31.7	25 – 46	28.3	8.4
Flo. Schools	US/ Florida	7	1	27.4	8 – 33	24.5	15.4
NRC. Retail	Canada	10	NA	31.4	18 – 44	49.3	19.6
Flo. Retail	US/ Florida	6	1	21.8	4 – 32	33.0	24.9
Industries	Suecia	9	NA	NA	NA	5.7	2.4
Flo. Industries	US/ Florida	9	1.1	24.9	4 - 57	41.4	26.6
Flo. Other	US/ Florida	25	NA	NA	NA	-	-
Other	Canada	1	5	10	10	-	-
Total		139				27.1	21.5

NA means that this information is not available for that group of buildings

From this study, Persily (1999) conclude that there is no correlation between the airtightness and the year of construction of the building or its age, that the wall construction did not have a significant influence over the airtightness and only frame walls appear to be somewhat leakier. With regards to the height, taller buildings appear to be tighter while shorter buildings covered the full spectrum of airtightness.

In relation to France, Litvak *et al*. (2001) have investigated the airtigthness of 12 non residential buildings (volume > 500m^3) less than 5 years old. They have analyzed the airtightness in relation to the construction type (metal/timber frame or concrete/masonry)

and their usage (hotels, schools, offices and polyvalent halls). Results of this work stated no influence of the construction type over the airtightness (expressed in terms of I_4), maybe because of the size of the sample. However, regarding the building activity different levels of airtightness performance were found, being hotels and scholar buildings tighter than office buildings and polyvalent halls (see Figure 2.5). These authors also reported that the level of performance of the airtightness appear to be influenced by the nature of the envelope leakage orifices, which seem to be larger than those of smaller buildings.

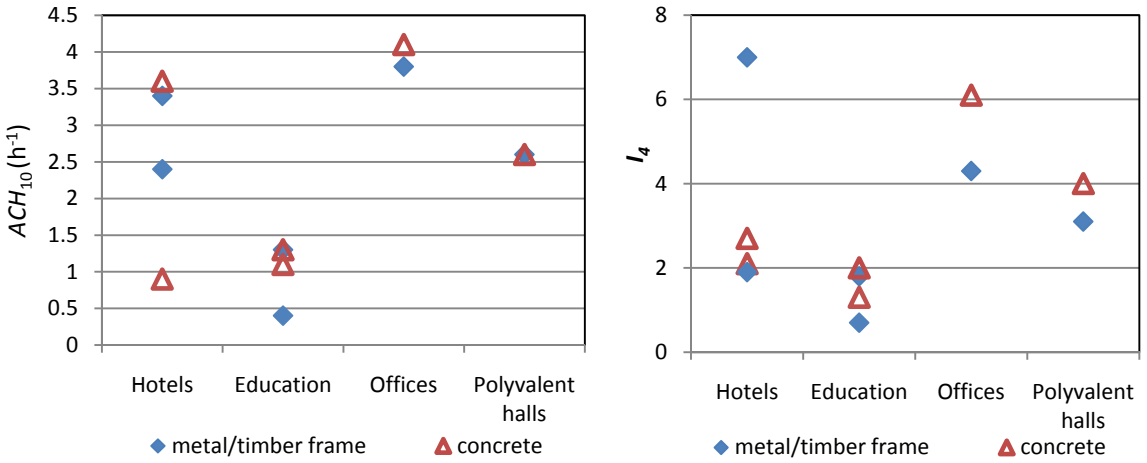

Figure 2.5 Airtightness of non residential building in France (Litvak *et al*., 2001)

A more recent work in this field is the one developed by the LBNL (Price *et al*., 2006), which comprises 267 data from non residential buildings in the US, Canada, Sweden, England and France, published in the literature. The authors analyze the airtightness of the buildings, expressed as the ratio between the ACH_{50} and the building envelope area, in relation to construction type (masonry, metal frame/panel, concrete panel), usage (offices, industrial/warehouses, schools, malls, recreational buildings, auditoriums, restaurants, supermarkets), year of construction (1960 to 2000), height (about 78% of the buildings were single story and only 6% were more than 5 stories) and footprint area (60% of the buildings have a footprint area lower than 1000 m^2). Results of this study show that there is little variation of the airtightness with construction type for a given building activity. However, for a given construction type schools and public assembly buildings seems to be tighter than average, while warehouses tend to be leakier. For a given usage and type of construction, buildings with smaller footprint areas (< 1000 m^2) seem to be 25% to 50% leakier, per unit of envelope area, than buildings with lager footprints; as well as higher buildings tend to be

tighter than shorter buildings. Concerning the age, these authors did not find any effect on the airtightness, as was also reported by Persily (1999).

2.4.4 Estimation of the *ACH* with tracer gases

The other way to determine the *ACH* of a building is to measure it. Direct measurements of the *ACH* are accomplished through a tracer gas dilution test described in the ASTM standard E741-00. This technique has been widely used (Smith, 1988; Persily, 1996; Blewett & Arca, 1999; ASHRAE, 2005; Jetter & Whitfield, 2005; Guo & Lewis, 2007) and is only applicable to spaces that are considered as single-zones (one volume), where indoor concentrations remains uniform. The test consist of the release of a tracer gas into a building in a specified manner, then, the tracer gas concentration within the building is monitored for a period of time, and finally, the measurements are related to the building air exchange rate through a mass balance. There are three different procedures reported in the standard: concentration decay, constant injection and constant concentration. The concentration decay consist on the injection of a small amount of tracer gas into the space, assuring that initial concentrations of the gas are uniform through the whole building, and then monitor the decay of the tracer gas concentration. In the constant injection procedure, the gas is injected uniformly into the zone, at a known constant rate, measurements of tracer gas concentrations are made at known times during the experiment. For the constant concentration technique, the tracer gas injection rate is adjusted to maintain a constant concentration within the building. From these procedures the concentration decay test is the simplest and most widely used. Gases used as tracers must have some characteristics like detectability, nonreactivity, nontoxicity, neutral buoyancy, relatively low concentration in ambient air and low cost (ASHRAE, 2005). Among the most used are sulphur hexafluoride (SF_6), carbon dioxide (CO_2), and perfluorocarbon compounds (PFTs).

In the three procedures, the *ACH* is determined through a mass balance as shown in Eq. 2.15. Then, if the gas used is not adsorbed onto surfaces and does not react with indoor compounds, the removal rate “R” is not considered. Based on this assumption, Table 2.15 presents the equations used in each procedure, according to the particular situation of each method.

Table 2.15 Equations for the tracer gas technique. (Guo & Lewis, 2007)

Concentration decay, S = 0

$$C_i(t) = C_o + (C_{i(t=0)} - C_o)\exp(-ACH \cdot t) \quad \text{Eq. 2.54}$$

Constant concentration, $\frac{dC_i}{dt} = 0$

$$ACH_o \cdot C_o - ACH_o \cdot C_i + \frac{S}{V} = 0 \quad \text{Eq. 2.55}$$

Constant emission, S = constant

$$C_i(t) = C_o + \frac{S}{V \cdot ACH} + \left(C_{i(t=0)} - C_o - \frac{S}{V \cdot ACH}\right)\exp(-ACH \cdot t) \quad \text{Eq. 2.56}$$

ACH Experimental data

Following the 1973 oil crisis, researchers in Germany and the Netherlands carried out a series of experimental *ACH* measurements as a step towards reducing ventilation heat losses (CPR 16E, 1989). The results of this research showed that *ACH* varied from 0.3 to 0.7 h^{-1} for high buildings and from 0.5 to 2.0 h^{-1} for low buildings, taking into account both multifamily and single-family dwellings (see Table 2.16). Two empirical expressions, shown in Eq. 2.57 and Eq. 2.58, were proposed for estimating the *ACH* as a function of wind speed. Engelmann (1992) examined previous *ACH* measurements of US dwellings and developed empirical isopleths to estimate *ACH* as a function of wind speed and temperature difference, for closed homes of modern construction with good insulation and for older homes with poor insulation.

Table 2.16 *ACH* for residences in Germany and the Netherlands (CPR16E, 1989)

Building type	***ACH*** **(h^{-1})**	**Year**	**Country**
Apartments	0.1 - 0.7	1977	The Netherlands
Maisonnettes	0.1 - 0.5	1978	The Netherlands
Single-family houses	0.9 - 1.7	1979	The Netherlands
Houses with good glass insulation	0.3 - 0.8	1983	Germany
For 80% of the number of houses tested	0.2 - 1.1	1983	Germany

High buildings $ACH\ (h^{-1}) = 0.1 + 0.04 \cdot v$ Eq. 2.57

Low buildings $ACH\ (h^{-1}) = 0.1 + 0.14 \cdot v$ Eq. 2.58

Murray and Burmaster (1995) and Angell *et al*. (2004) studied the *ACH* distribution of single-family dwellings in the US as a function of climatic region and season. They found that for all regions and seasons, most of the *ACH*s lied between 0.21 and 1.55 h^{-1}, 10^{th} and 90^{th} percentiles, respectively (see Table 2.17). They also reported *ACH*s lower than 0.5 h^{-1} for 60% of dwellings in winter, 50% in spring, 80% in autumn and only 25% in summer. This result for summer is unusual since lower *ACH* are expected if windows and doors are closed, however the authors stated no knowledge about the status of the openings from the data analyzed.

Table 2.17 Statistics for Residential Ventilation Rates in the US (Pandian *et al*., 1998; Angell *et al*., 2004)

Sample	Number	GM	GSD	10%	25%	50%	75%	90%
Regions, all seasons North								
East	842	0.42	2.19	0.17	0.29	0.42	0.66	1.01
North West	585	0.33	1.88	0.16	0.22	0.33	0.48	0.68
South East	62	0.61	2.89	0.19	0.35	0.62	0.95	1.94
South West	1482	0.71	2.25	0.29	0.42	0.67	1.14	1.76
Season, all regions								
All US, Dec, Jan, Feb	1162	0.43	2.05	0.19	0.30	0.42	0.66	0.97
All US, Mar, Apr, May	1160	0.51	2.17	0.21	0.32	0.53	0.82	1.22
All US, Jun, Jul, Aug	507	0.99	2.56	0.35	0.53	0.99	1.93	2.79
All US, Sep, Oct, Nov	142	0.35	1.96	0.16	0.23	0.37	0.49	0.75
All regions, all seasons	2971	0.53	2.31	0.21	0.32	0.50	0.85	1.55

GM: geometric mean (h^{-1})
GSD: geometric standard deviation (h^{-1})

Figure 2.6 shows a histogram of the air infiltration frequency of a sample of North American houses presented in the ASHRAE handbook (2005), where most of the data (75%) lied between 0.25 and 0.75 h^{-1}.

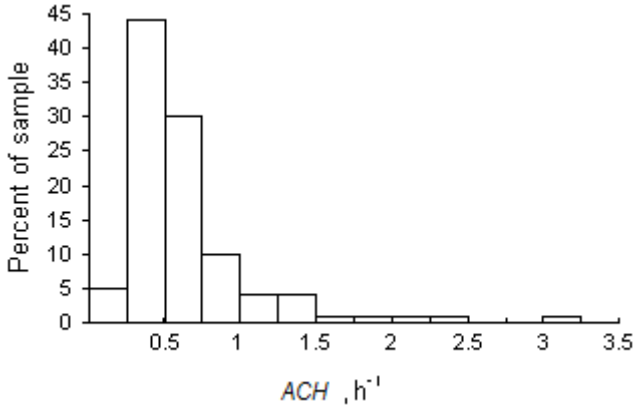

Figure 2.6 *ACH* distribution in North America dwellings (ASHRAE, 2005).

The TNO (CPRE16, 1989) has also reported some data concerning the relation of the *ACH* with the state of doors and windows (Table 2.18). This type of ventilation, with doors and windows opened, is important in the final stage of shelter-in-place since it determines the decrease of the indoor concentration after the cloud passed.

Table 2.18 Relationship between *ACH* and the condition of windows and doors (CPRE16E, 1989)

Windows/doors condition	***ACH*** **(h^{-1})**
Windows and doors closed	0 - 0.5
Windows ajar	0.8 -4.0
Windows half open	5 -10.0
Windows fully open	9.0 - 15
Windows and doors open against each other	40

Guo and Lewis (2007) developed an interesting work that consists of determining the *ACH* of six Irish single-family dwellings. To accomplish this, they used the pressurization technique to determine the airtightness (ACH_{50}), the tracer gas technique with SF_6 to estimate the *ACH* of the whole dwelling and the metabolic CO_2 concentration measured in an occupied room. They monitored the CO_2 concentration continuously for 2 to 7 days in order to calculate the *ACH* based on a mass balance. These authors support the selection of a bedroom to represent the whole house *ACH* (using the metabolic CO_2), on the assumption that a small-scale enclosure inside the dwelling can represent the infiltration and ventilation performance of the whole structure. To analyze the *ACH* with CO_2, the authors took the average of the *ACHs* found every night during the steadily increasing periods of the CO_2 concentration, using Eq. 2.56. From the results reported by these authors (Table 2.19), the highest correlation (87%) was found

between ACH_{CO2} and the ACH_{50}, while for ACH_{CO2} and ACH_{SF6} it was 68%, and for ACH_{SF6} and ACH_{50} 63%. Concerning the results with CO_2 and SF_6, similar values were obtained with differences lower than 12% (based on the SF_6 results), except for dwelling number 3 which exhibits a difference of 25%.

Table 2.19 *ACH* of different Irish dwellings (Guo & Lewis, 2007)

Dwelling	ACH_{CO2} (h^{-1})	ACH_{SF6} (h^{-1})	ACH_{50} (h^{-1})
1	1.07	1.22	12.43
2	0.97	0.98	13.47
3	1.43	1.14	16.66
4	1.22	1.28	16.29
5	0.97	0.9	10.86
6	0.92	0.83	12.5

2.5 Methodology used by the Catalan Government to establish the evacuation radius

Catalan Government estimates shelter-in-place effectiveness with the aim of establishing the evacuation radius in the case of a toxic gas release. Currently, industries that manage hazardous substances in quantities above the thresholds stated by the Spanish regulations (Real Decret 1254/1999) must provide an analysis of risk where interventions zones are defined. Intervention zones established by the Spanish regulation (Real Decret 1196/2003), in the case of a toxic gas release, consider the alert and the intervention zone as mentioned in section 1.2. In addition to these zones Catalan Government defines the LC01 and the evacuation zone. The first one involves the area in which 1% casualties are expected outside, while the second refers to the area in which 0.1% casualties are expected indoors when shelter-in-place is implemented (PLASEQCAT, 2007). The estimation of a percentage of casualties in these situations is achieved using the Probit functions (Eq. 2.2 and Eq. 2.3).

Therefore, the methodology currently used in Catalunya to determine the evacuation radius, given an external concentration, consists of the following steps (PLASEQCAT, 2007):

1. Estimate the indoor concentration at different distances with Eq. 2.59, using a fixed *ACH*. The latest criteria published by the Catalan Government stated that a value between 2 and

5 h^{-1} should be used (PLASEQCAT, 2007), but no guidance is provided on how to chose this value. However, the previous version of the PLASEQCAT (2005) mentions that an *ACH* of 2 h^{-1} might be used.

$$\frac{C_i}{C_o} = 1 - \frac{1 - \exp(-ACH \cdot t)}{ACH \cdot t} \quad \text{Eq. 2.59}$$

2. Calculate the TL_i assuming a constant indoor concentration for each distance (Eq. 2.60).

$$TL_i = C_i^n \cdot t \quad \text{Eq. 2.60}$$

3. Estimate P_r using Eq. 2.2 and P from Eq. 2.3.

4. The distance at which P equals 0.001 is considered the evacuation radius.

The equation used by the Catalan Government to relate outdoor to indoor concentration (Eq. 2.59) corresponds to the equation reported by Lees (1996) to relate the indoor and outdoor toxic loads, when n = 1 and the outdoor concentration behaviour is represented by a block function, as in Eq. 2.30. Therefore, the application of this equation leads to an average indoor concentration that would give the same TL_i if the toxic load exponent is equal to 1 (n = 1). However, if the n is different ($n \neq 1$), the TL_i is expected to be underestimated ($n > 1$) or overestimated ($n < 1$), leading to an under or overestimation of the evacuation radius, respectively.

Chapter 3. Analysis of the parameters involved in the estimation of shelter-in-place effectiveness

"The mark of a great faith is not liberation, but faithfulness in the midst of difficulties"
Lindsay Brown

The aim of this chapter is to analyze the effect that the different parameters and models have on the estimation of shelter-in-place effectiveness. The first part presents the analytical solutions to calculate indoor concentration, when sorption takes place, in the case of continuous and temporary sources assuming an outdoor concentration given by the Gaussian dispersion model. Then, an analysis of the performance of these models was done. The second part, deals with a sensitivity analysis to evaluate the influence of different parameters on the TL_i and *TLRF*. Finally, we performed a comparison of the methodology used by the Catalan Government to estimate the evacuation radius using different substances. A parallel analysis based on the estimation of SF_i, using the AEGL-3 was also developed, in order to confirm the results obtained.

3.1 Estimation of C_i considering adsorption/desorption processes

Regarding the estimation of indoor concentration assuming a Gaussian outdoor dispersion (Eq. 2.28) and considering adsorption/desorption processes over indoor materials, analytical solutions were obtained for the cases of continuous and temporary sources. Analytical solutions are preferred over numerical solutions, since they are explicit, easier to manage and the results are free of numerical approximations. The time-dependent solution to the differential equations that represent the three types of sink models (Eq. 2.24 – 2.26) with j = 1, were obtained using the method of undetermined coefficients (Zill, 1988), depending on initial conditions, as explained below.

Continuous source

For a continuous source, the solution to the set of differential equations with initial conditions $C_i(0) = m_1(0) = m_2(0) = 0$ is represented by the exponential functions given in Eq. 3.1 to Eq. 3.3:

$$C_i = d_1 \cdot x_{11} \exp(\lambda_1 \cdot t) + d_2 \cdot x_{12} \exp(\lambda_2 \cdot t) + d_3 \cdot x_{13} \exp(\lambda_3 \cdot t) + a_1 \quad \text{Eq. 3.1}$$

$$m_1 = d_1 \cdot x_{21} \exp(\lambda_1 \cdot t) + d_2 \cdot x_{22} \exp(\lambda_2 \cdot t) + d_3 \cdot x_{23} \exp(\lambda_3 \cdot t) + a_2 \quad \text{Eq. 3.2}$$

$$m_2 = d_1 \cdot x_{31} \exp(\lambda_1 \cdot t) + d_2 \cdot x_{32} \exp(\lambda_2 \cdot t) + d_3 \cdot x_{33} \exp(\lambda_3 \cdot t) + a_3 \quad \text{Eq. 3.3}$$

In these equations λ_1, λ_2 and λ_3 are the eigenvalues of the coefficient matrix and are given by the roots of the cubic or quadratic equation; x_{ij} are the coefficients of the eigenvector matrix (X); a_1, a_2 and a_3 are the solutions to the homogeneous system; and d_1, d_2 and d_3 are the constants determined by the initial conditions. Table 3.1 gives expressions for these parameters depending on the model used.

Temporary source

As for a temporary source the outdoor concentration is represented by the block function (Eq. 2.30), the indoor concentration for the lapse of time where $0 \leq t \leq t_1$ is the same as for a continuous source Eq. 3.1 to Eq. 3.3. However, after the plume passed ($t > t_1$), C_o becomes 0 and other initial conditions should be used to solve the differential equations, equal to the

Table 3.1 Solution parameters for a continuous source using sink models.

Parameter	One-sink model	Sink-diffusion model	Two-sink model
$\lambda_1, \lambda_2, \lambda_3$	$\lambda^2 + \lambda \cdot \left(k_d + ACH + k_a \cdot \frac{A}{V} \right) +$ $ACH \cdot k_d = 0$	$\lambda^3 + \lambda^2 \cdot \left(2 \cdot k_{dif} + k_d + k_a \cdot \frac{A}{V} + ACH \right) + \lambda \cdot$ $\left(k_{dif} \cdot \left(k_d + 2 \cdot ACH + 2 \cdot k_a \cdot \frac{A}{V} \right) + ACH \cdot k_d \right) +$ $ACH \cdot k_{dif} \cdot k_d = 0$	$\lambda^3 + \lambda^2 \cdot \left(k_d + k_1 + k_2 + k_a \cdot \frac{A}{V} + ACH \right) +$ $\lambda \cdot \left(k_2 \cdot k_d + ACH \cdot (k_d + k_1 + k_2) + k_a \cdot \frac{A}{V} \cdot (k_1 + k_2) \right) +$ $ACH \cdot k_2 \cdot k_d = 0$
x_{ij}	$x_{11} = 1; \quad x_{12} = 1;$ $x_{21} = \frac{k_a}{k_d + \lambda_1}; \quad x_{22} = \frac{k_a}{k_d + \lambda_2}$	$x_{11} = 1; \quad x_{12} = 1; \quad x_{13} = 1;$ $x_{21} = \frac{\lambda_1 + ACH + k_a \cdot A/V}{k_d \cdot A/V}; \quad x_{22} = \frac{\lambda_2 + ACH + k_a \cdot A/V}{k_d \cdot A/V};$ $x_{23} = \frac{\lambda_3 + ACH + k_a \cdot A/V}{k_d \cdot A/V}$ $x_{31} = \frac{k_{dif} \cdot x_{21}}{\lambda_1 + k_{dif}}; \quad x_{32} = \frac{k_{dif} \cdot x_{22}}{\lambda_2 + k_{dif}}; \quad x_{33} = \frac{k_{dif} \cdot x_{23}}{\lambda_3 + k_{dif}}$	$x_{11} = 1; \quad x_{12} = 1; \quad x_{13} = 1;$ $x_{21} = \frac{\lambda_1 + ACH + k_a \cdot A/V}{k_d \cdot A/V}; \quad x_{22} = \frac{\lambda_2 + ACH + k_a \cdot A/V}{k_d \cdot A/V};$ $x_{23} = \frac{\lambda_3 + ACH + k_a \cdot A/V}{k_d \cdot A/V}$ $x_{31} = \frac{k_1 \cdot x_{21}}{\lambda_1 + k_2}; \quad x_{32} = \frac{k_1 \cdot x_{22}}{\lambda_2 + k_2}; \quad x_{33} = \frac{k_1 \cdot x_{23}}{\lambda_3 + k_2}$
a_1	C_o	C_o	C_o
a_2	$C_o \cdot \frac{k_a}{k_d}$	$C_o \cdot \frac{k_a}{k_d}$	$C_o \cdot \frac{k_a}{k_d}$
a_3		$C_o \cdot \frac{k_a}{k_d}$	$C_o \cdot \frac{k_1}{k_2} \cdot \frac{k_a}{k_d}$
d_1	$C_o \cdot \frac{k_a/k_d - x_{22}}{x_{22} - x_{21}}$	$C_o \cdot \frac{(k_a/k_d) \cdot (x_{33} + x_{22} - x_{32} - x_{23}) - x_{22} \cdot x_{33} + x_{32} \cdot x_{23}}{\det X}$	$C_o \cdot \frac{(k_a/k_d) \cdot (x_{33} - x_{32} + k_1/k_2 \cdot (x_{22} - x_{23})) - x_{22} \cdot x_{33} + x_{32} \cdot x_{23}}{\det X}$
d_2	$C_o \cdot \frac{x_{21} - k_a/k_d}{x_{22} - x_{21}}$	$C_o \cdot \frac{(k_a/k_d)(x_{31} - x_{33} - x_{21} + x_{23}) - x_{31} \cdot x_{23} + x_{21} \cdot x_{33}}{\det X}$	$C_o \cdot \frac{(k_a/k_d) \cdot (x_{31} - x_{33} + k_1/k_2 (x_{23} - x_{21})) - x_{31} \cdot x_{23} + x_{21} \cdot x_{33}}{\det X}$
d_3		$C_o \cdot \frac{(k_a/k_d) \cdot (x_{32} + x_{21} - x_{22} - x_{31}) - x_{21} \cdot x_{32} + x_{31} \cdot x_{22}}{\det X}$	$C_o \frac{(k_a/k_d) \cdot (x_{32} - x_{31} + k_1/k_2 \cdot (x_{21} - x_{22})) - x_{21} \cdot x_{32} + x_{31} \cdot x_{22}}{\det X}$
det X	$x_{22} - x_{21}$	$x_{21} \cdot (x_{32} - x_{33}) + x_{22} \cdot (x_{33} - x_{31}) + x_{23} \cdot (x_{31} - x_{32})$	$x_{21} \cdot (x_{32} - x_{33}) + x_{22} \cdot (x_{33} - x_{31}) + x_{23} \cdot (x_{31} - x_{32})$

values obtained for C_i, m_1 and m_2 at $t = t_1$ with Eq. 3.1 to Eq. 3.3 ($C_{i,t1}$, $m_{1,t1}$ and $m_{2,t1}$). The solution with these initial conditions is given by the following expressions:

$$C_i(t > t_1) = p_1 \cdot x_{11} \exp(\lambda_1 \cdot t) + p_2 \cdot x_{12} \exp(\lambda_2 \cdot t) + p_3 \cdot x_{13} \exp(\lambda_3 \cdot t) \quad \text{Eq. 3.4}$$

$$m_1(t > t_1) = p_1 \cdot x_{21} \exp(\lambda_1 \cdot t) + p_2 \cdot x_{22} \exp(\lambda_2 \cdot t) + p_3 \cdot x_{23} \exp(\lambda_3 \cdot t) \quad \text{Eq. 3.5}$$

$$m_2(t > t_1) = p_1 \cdot x_{31} \exp(\lambda_1 \cdot t) + p_2 \cdot x_{32} \exp(\lambda_2 \cdot t) + p_3 \cdot x_{33} \exp(\lambda_3 \cdot t) \quad \text{Eq. 3.6}$$

Since the homogeneous system remains unchanged, the eigenvalues and eigenvectors are the same as in the continuous case (Table 3.1). Table 3.2 shows the constants given by the initial conditions (p_1, p_2 and p_3) for each model.

Table 3.2 Solution constants for a temporary source using sink models ($t > t_1$).

Model	**p_1, p_2 and p_3**
One-sink	$p_1 = \frac{\left[C_{i,t1} \cdot x_{22} - m_{1,t1}\right]}{e^{t_1\lambda_1} \cdot (x_{22} - x_{21})}$; $p_2 = \frac{m_{1,t1} - C_{i,t1} \cdot x_{21}}{e^{t_1\lambda_2} \cdot (x_{22} - x_{21})}$
Sink-diffusion and Two-sink	$p_1 = \frac{e^{t_1(\lambda_2+\lambda_3)}\left[C_{i,t1} \cdot (x_{22} \cdot x_{33} - x_{32} \cdot x_{23}) + m_{1,t1} \cdot (x_{32} - x_{33}) + m_{2,t1} \cdot (x_{23} - x_{22})\right]}{e^{t_1(\lambda_1+\lambda_2+\lambda_3)} \det X}$
	$p_2 = \frac{e^{t_1(\lambda_1+\lambda_3)}\left[C_{i,t1} \cdot (x_{31} \cdot x_{23} - x_{21} \cdot x_{33}) + m_{1,t1} \cdot (x_{33} - x_{31}) + m_{2,t1} \cdot (x_{21} - x_{23})\right]}{e^{t_1(\lambda_1+\lambda_2+\lambda_3)} \det X}$
	$p_3 = \frac{e^{t_1(\lambda_1+\lambda_2)}\left[C_{i,t1} \cdot (x_{21} \cdot x_{32} - x_{31} \cdot x_{22}) + m_{1,t1} \cdot (x_{31} - x_{32}) + m_{2,t1} \cdot (x_{22} - x_{21})\right]}{e^{t_1(\lambda_1+\lambda_2+\lambda_3)} \det X}$

3.1.1 Behavior of indoor concentration models

In order to compare the behavior of the models presented to relate outdoor to indoor concentration assuming a Gaussian outdoor dispersion and a temporary source, we analyzed the change in the indoor concentration given by each model: no adsorption (Eq. 2.37), constant adsorption (Eq. 2.37 and Eq. 2.38), one-sink (Eq. 3.1, Eq. 3.2, Eq. 3.4 and Eq. 3.5), sink-diffusion and two-sink models (Eq. 3.1 to Eq. 3.6). We used the adsorption parameters of chlorine and the DMMP (a surrogate of the nerve agent sarin) to assess the adsorption models. For the analysis, a house located 500 m downwind from the release was considered and two

ACH, 0.5 and 1h^{-1}, were evaluated in order to assess the influence of this parameter. These values were chosen since they are typical values reported in experimental data (see section 2.4.4). Table 3.3 presents the other conditions used in the calculation.

Table 3.3 Conditions used to evaluate the models to relate outdoor to indoor concentration

Parameter	Value	Parameter	Value
x (m)	500	Stability	D
y (m)	0	v ($m \cdot s^{-1}$)	5
z (m)	2	ACH (s^{-1})	$1.38 \cdot 10^{-4}$, $2.78 \cdot 10^{-4}$ (0.5, 1 h^{-1})
h (m)	0	A/V (m^{-1})	3.5
z_o (m)	0.1	$\dot{q}$ ($kg \cdot s^{-1}$)	0.5
t_1 (s)	1800		

Figure 3.1 shows the changes in indoor concentration of chlorine for the models without adsorption, with constant adsorption and the one-sink model, respectively. The parameters needed for these models were taken as the average of the values presented in Table 2.2 and Table 2.3 for Cl_2. This figure shows that adsorption greatly lowers indoor concentration. With respect to the model without adsorption, the reduction was on the order of 25% with the constant adsorption model and 32% with the one-sink model (based on maximum concentrations). Reductions in indoor concentration in relation to outdoor concentration, for the model without adsorption, depend on *ACH* and become greater as *ACH* decreases. At higher *ACH*, the concentration decay becomes faster after the end of the release. In both situations, the adsorption models reach the same concentrations 2 h after the end of the release and show the same behavior after that time. The final concentration for the model without adsorption at an *ACH* of 1 h^{-1} is 50% lower than that reached with 0.5 h^{-1}.

For DMMP, the purpose was to compare indoor concentration behavior when using the adsorption parameters for the one-sink, sink-diffusion and two-sink models reported in different situations (Table 2.4): a room with aged wallboard, plush and hard furnishings (Figure 3.2), and a residential room (Figure 3.3).

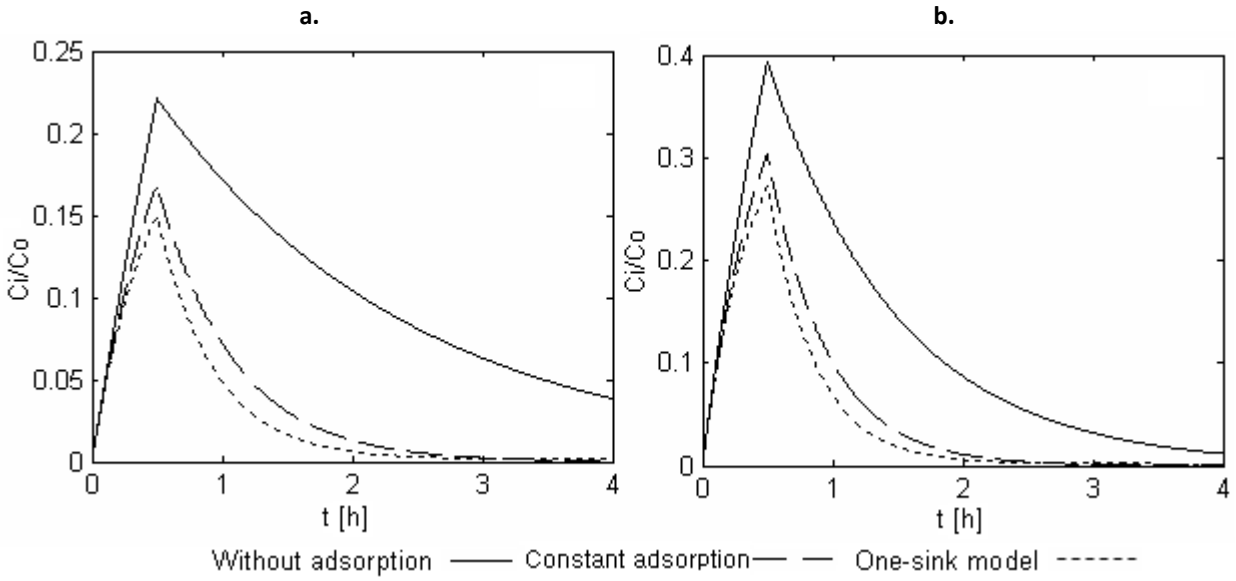

Figure 3.1 Indoor concentration of Cl_2. a) *ACH*=0.5 h^{-1}, b) *ACH*=1 h^{-1}.

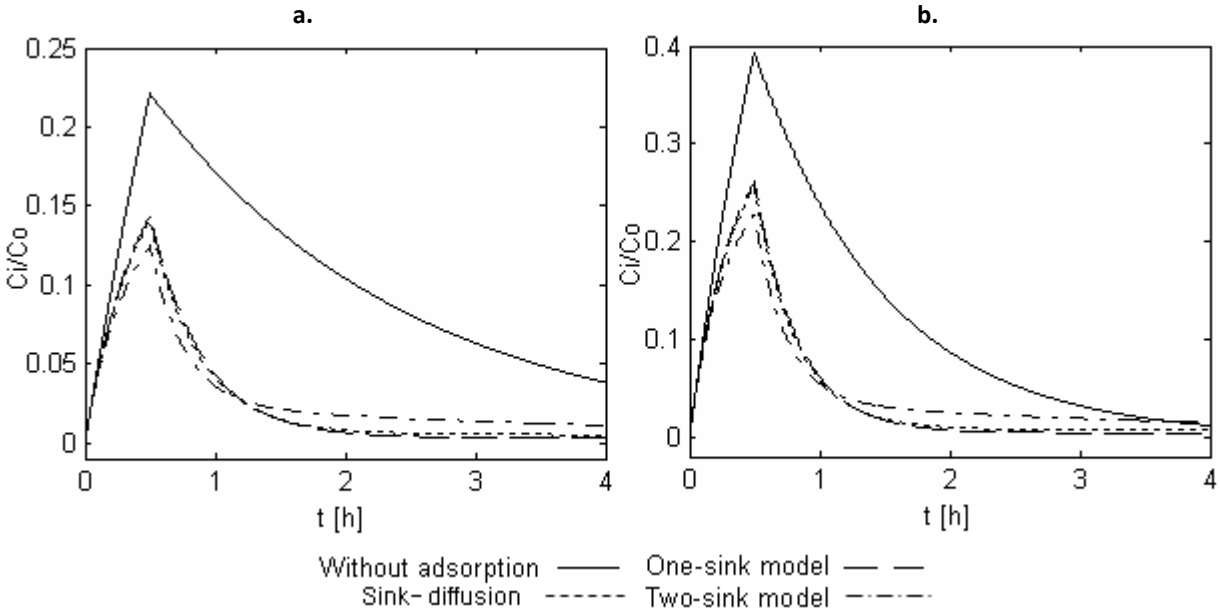

Figure 3.2 Indoor concentration of DMMP for a room with aged wallboard, plush and hard furnishings. a) *ACH*=0.5 h^{-1}, b) *ACH*=1 h^{-1}.

The two figures show that the one-sink and sink-diffusion models have very similar behavior, following almost the same concentrations. The two-sink model differs more from this behavior, especially in the room with aged wallboard, where the final indoor concentration remains higher than the concentrations obtained with the other adsorption models, and equal to that of the model without adsorption for an air infiltration frequency of 1 h^{-1} (Figure 3.2b). This could be due to a slow mass transfer mechanism to the embedded sink (see Figure 3.4), which would allow a residual indoor concentration over a long period. In the case of a

residential room, the indoor concentration and the mass on the surface (m_1) decay more quickly after the end of the release due to the high rate of mass transfer to the embedded sink. Thus, the mass stored in this sink (m_2) exceeds the mass on the surface, as shown in Figure 3.4.

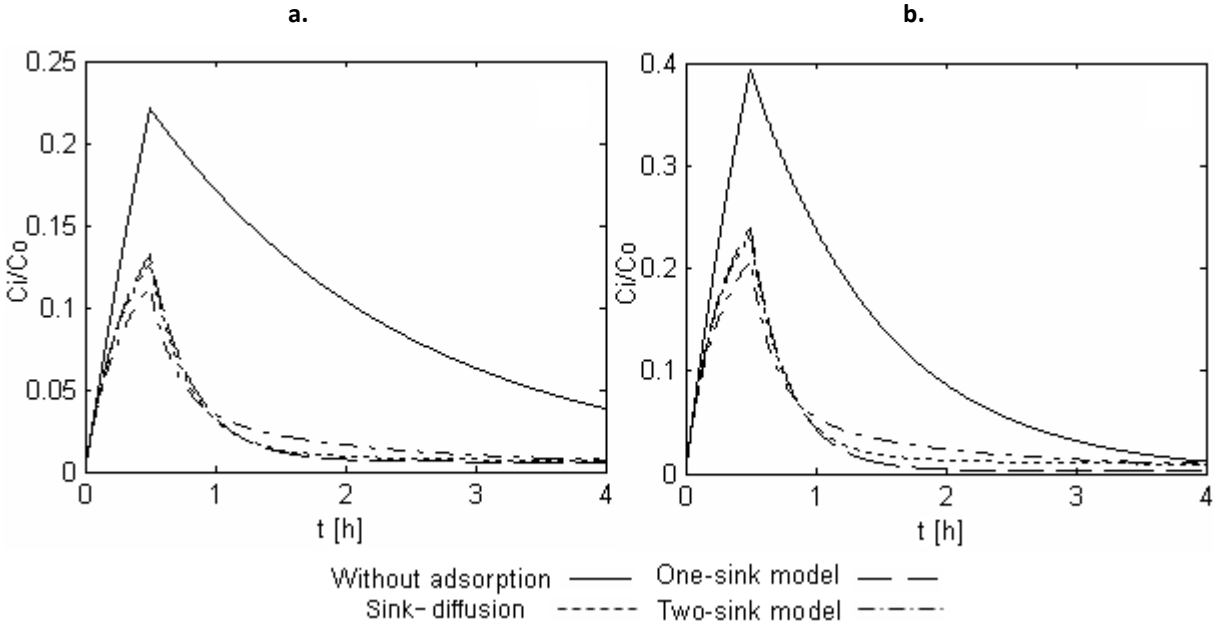

Figure 3.3 Indoor concentration of DMMP for residential room. a) *ACH*=0.5 h^{-1}, b) *ACH*=1 h^{-1}.

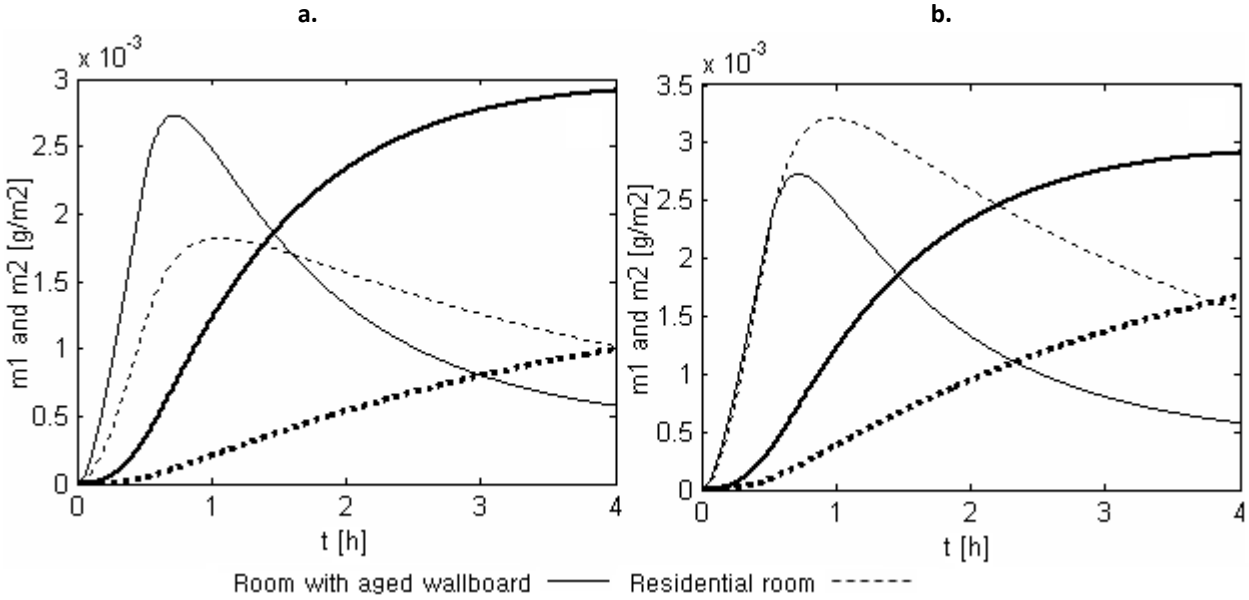

Figure 3.4 DMMP mass on the surface "m_1" (thin lines) and internal sink "m_2" (heavy lines) obtained with the two-sink model. a) *ACH*=0.5 h^{-1}, b) *ACH*=1 h^{-1}.

The reduction in DMMP concentration achieved by means of adsorption with respect to the model without adsorption ranges from 40 to 51% in the case of a residential room, and from 35 to 44% in the case of a room with aged wallboard. Therefore, a substantial reduction on indoor concentration could be achieved if the substance involved can be adsorbed onto surfaces; however the use of one or another model is conditioned by the availability of adsorption/desorption parameters, which are scarce in the literature. Table 3.4 present the maximum indoor concentration reduction achieved when sorption processes take place with regards to the situation of non adsorption, for the cases analyzed in Figure 3.1 to Figure 3.3.

High-adsorptive materials with high mass transfer rates lead to a significant initial decrease in indoor concentration due to an increase in the mass contained in the embedded sink (Figure 3.2 - Figure 3.4). However, these materials may act as re-emitting sources and cause an increase in the retention time of the substance in the indoor environment. It is therefore very important to establish an appropriate termination time for sheltering in order to avoid prolonged exposure.

Table 3.4 Maximum indoor concentration reduction with regards to the case without adsorption

Situation	Maximum reduction on C_i (%)
Deposition model, Cl_2 adsorption parameters	25
One-sink, Cl_2 adsorption parameters	32
One-sink, DMMP parameters (Room with aged wallboard)	35
Sink-diffusion, DMMP parameters (Room with aged wallboard)	37
Two-sink, DMMP parameters (Room with aged wallboard)	44
One-sink, DMMP parameters (Residential room)	40
Sink-diffusion, DMMP parameters (Residential room)	42
Two-sink, DMMP parameters (Residential room)	51

3.2 Sensitivity analysis

The sensitivity analysis presented in this section is based on two criteria. The first part deals with the assessment of the TL_i and the *TLRF* as shelter-in-place effectiveness indicators, while the second part is focused on the estimation of the evacuation radius.

3.2.1 Based on the TL_i and the *TLRF*

To assess the influence that variables like the release characteristics, substance type or meteorological conditions, have on the assessment of shelter-in-place effectiveness, represented by the TL_i and *TLRF*, we defined a base case with standard values for the variables involved (Table 3.5) from which they were later varied. Variables considered in this analysis comprise the model used to estimate indoor concentration, type of substance, *ACH*, release duration, magnitude of the emission and atmospheric stability.

Table 3.5 Base case conditions

Parameter	Value	Parameter	Value
x (m)	500	Stability	D
y (m)	0	v ($m \cdot s^{-1}$)	5
z (m)	2	Model	Without adsorption
h (m)	0	n	2
z_o (m)	0.01	ACH (s^{-1})	$1.38 \cdot 10^{-4}$ ($0.5\ h^{-1}$)
t_1 (h)	0.5	A/V (m^{-1})	3.5
$\dot{q}$ ($kg \cdot s^{-1}$)	0.5		

The influence of indoor concentration models, refers to the influence that adsorption/ desorption processes have on the TL_i and *TLRF*. Table 3.6 presents the values for the adsorption/desorption parameters used by each model. The type of substance involved was defined according to the toxic load exponent "*n*", which took three values: 1, 2 and 3. For the *ACH* we considered 0.5, 1 and 2 h^{-1}, which are common values in single-family dwellings. Concerning the emission characteristics, the release duration was taken as 0.1, 0.5 and 2 h; and the magnitude of the emission as 1, 100 and 1000 kg. Regarding the atmospheric stability, three situations were evaluated: neutral (v = 5 $m \cdot s^{-1}$), unstable (v = 3 $m \cdot s^{-1}$) and stable (v = 3 $m \cdot s^{-1}$). We used the temporary source described by the Gaussian model to estimate outdoor concentration (Eq. 2.31 and Eq. 2.32).

Influence of adsorption/desorption processes

Evaluating the influence of the adsorption/desorption processes we find two trends, independently of the substance type, depending on the presence or not of adsorption (Figure 3.5). This behavior is also associated with the evolution of C_i, which is clearly reduced due to

Table 3.6 Parameters used for the adsorption/desorption indoor concentration models

Model	Parameter	Value
Constant adsorption[a]	v_d ($m \cdot s^{-1}$)	$1.4 \cdot 10^{-4}$
One sink[b]	k_a ($m \cdot s^{-1}$)	$1.944 \cdot 10^{-4}$
	k_d (s^{-1})	$2.5 \cdot 10^{-5}$
Sink-diffussion[b]	k_a ($m \cdot s^{-1}$)	$2.1388 \cdot 10^{-4}$
	k_d (s^{-1})	$4.7222 \cdot 10^{-5}$
	k_{dif}	$5.8333 \cdot 10^{-5}$
Two-sink[b]	k_a ($m \cdot s^{-1}$)	$3.0555 \cdot 10^{-4}$
	k_d (s^{-1})	$2.3888 \cdot 10^{-4}$
	k_1 (s^{-1})	$2 \cdot 10^{-4}$
	k_2 (s^{-1})	$3.333 \cdot 10^{-5}$

[a] Common value for organic gases in rooms (Singer *et al*. 2004)
[b] Values for DMMP in a residential room (Singer *et al*. 2005b)

adsorption (Figure 3.6). All the cases where adsorption take place have lower TL_i and higher *TLRF* than when no adsorption is present; this represents a substantial reduction of the TL_o due to shelter-in-place and adsorption processes. Nevertheless, the effect of adsorption is more visible for cumulative substances (n = 1) than for peak substances (n > 1), which have a high *TLRF* even when no adsorption is present, due to the reduction of the peak concentration as mentioned in section 2.1. For n = 1, the TL_i clearly increases with time (Figure 3.5.a), however, when adsorption take place this behavior is lessen since C_i diminishes quickly in comparison with the non-adsorption situation (Figure 3.6.a.).

We can also see that when adsorption is present the TL_i stabilizes quickly (especially for n > 1) after the passage of the plume, therefore shelter-in-place effectiveness becomes independently of shelter duration. By contrast, in the case of non adsorption, the TL_i increases with time (particularly for cumulative substances) and the shelter duration becomes an important parameter for shelter success. This situation is also reflected on the behavior of the SF_i in Figure 3.7, where for peak substances this indicator remains almost the same with time, while for cumulative substances it decreases, being less the effect when adsorption is present. In relation to the *TLFR* assessed at 2 h, it decreases by around 50%, 7% and 1% when non adsorption takes place with regards to the situation when substances sorbs, for the cases of n = 1, 2 and 3, respectively.

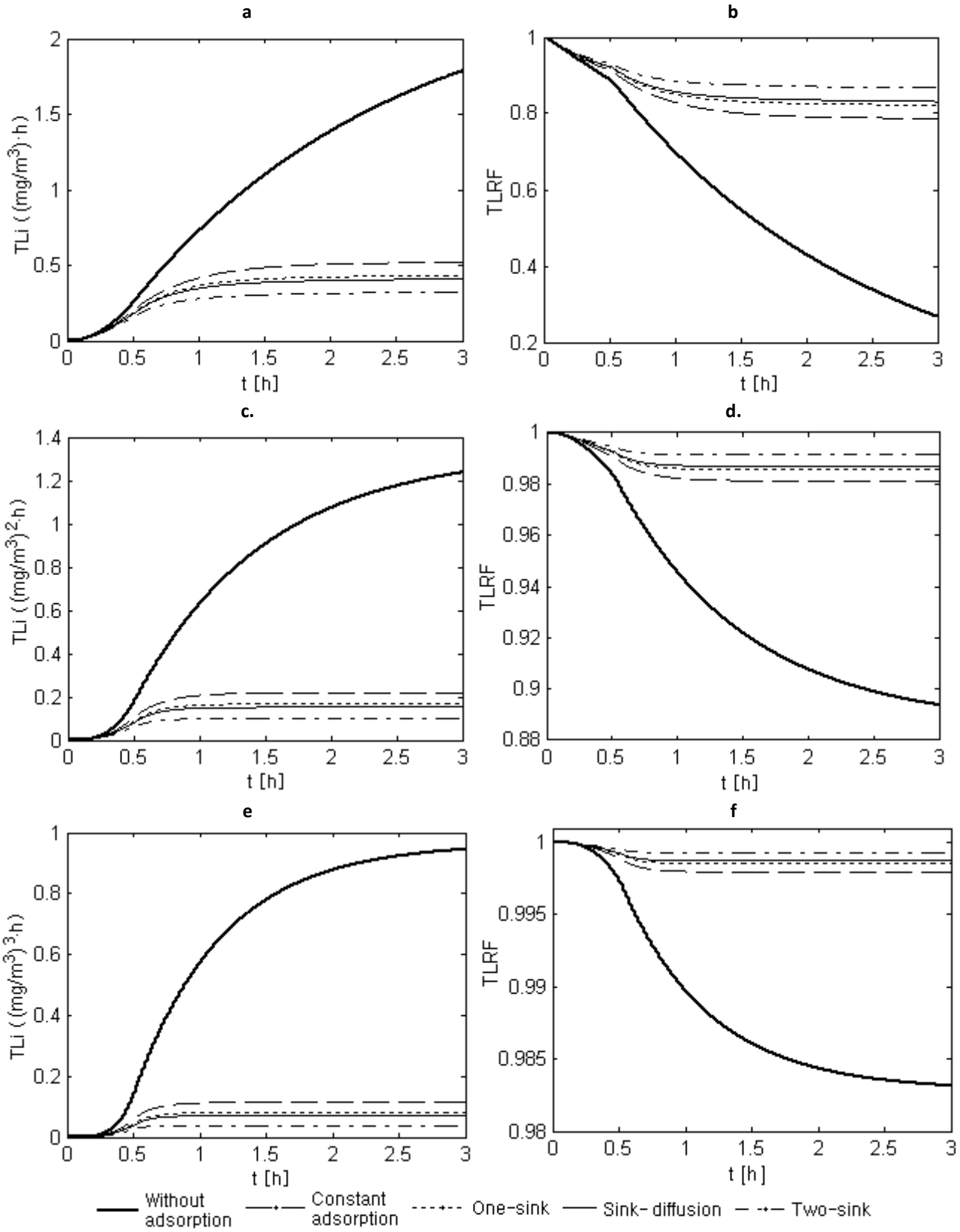

Figure 3.5 Influence of the type of substance and adsorption/desorption processes on the TL_i and the *TLRF* for *n*=1 (a, b), *n*=2 (c, d) and *n*=3 (e, f)

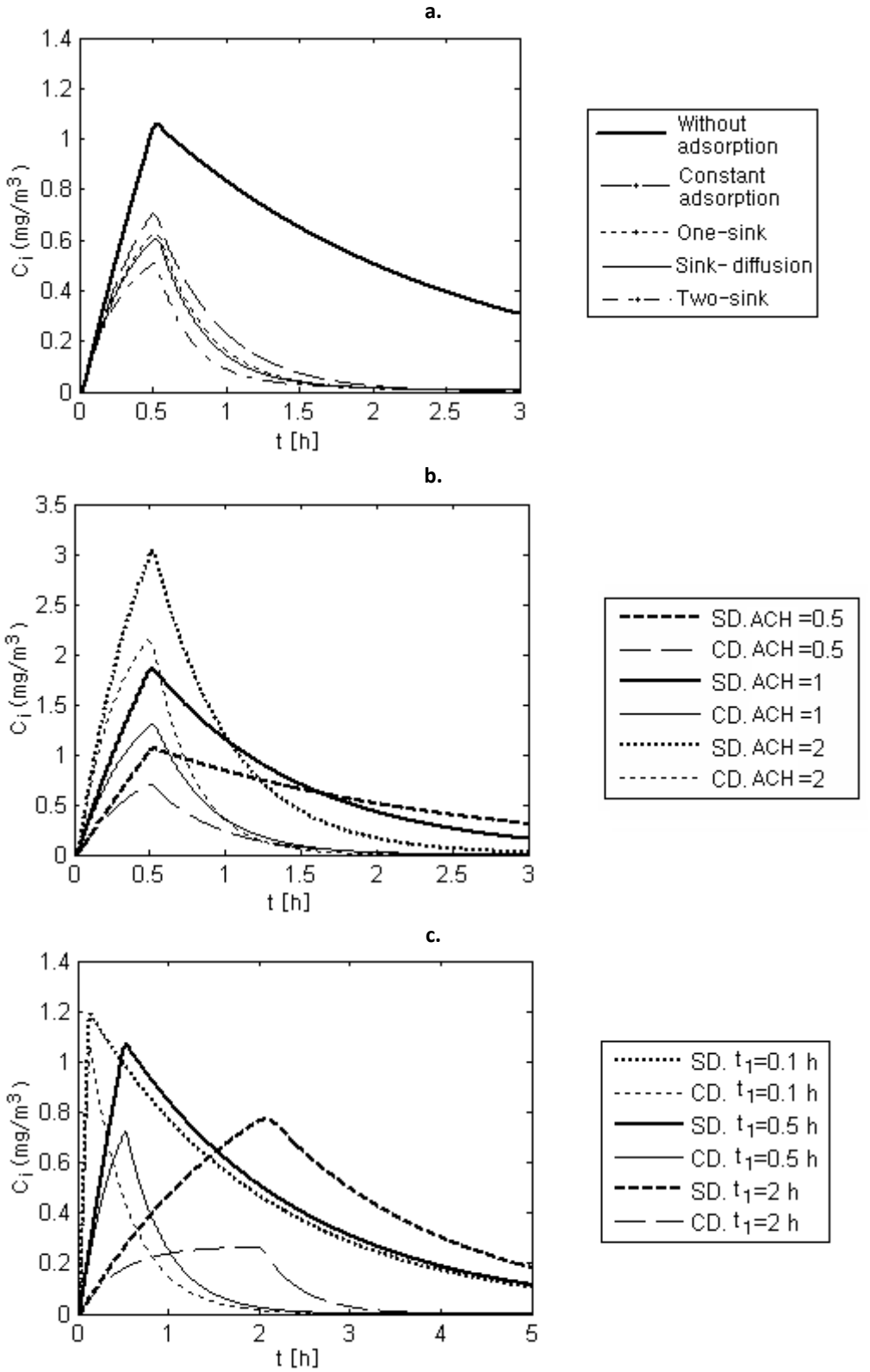

Figure 3.6 Indoor concentration. SD: without adsorption CD: constant adsorption. a) Influence of adsorption/desorption processes, b) Influence of the *ACH*, c) Influence of release time

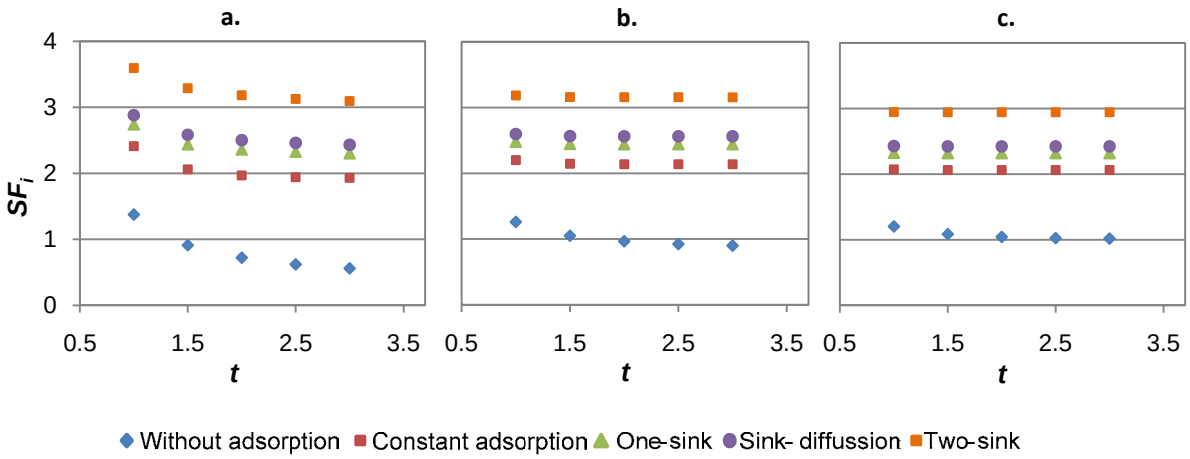

Figure 3.7 Influence of the type of substance and adsorption/desorption processes on the SF_i. a) n=1, b) n=2, c) n=3

As the models that include adsorption processes (constant adsorption, one-sink, sink-diffusion and two-sink) follow the same trend, as well as substances with n = 2 and n = 3, we decided to consider only the constant adsorption case (in representation of the adsorption processes) and the toxic load exponents 1 and 2 for the following analysis.

Influence of the ACH

For substances with n = 2 (in general n > 1), the *ACH* has a great influence over the TL_i and the *TLRF*. Figure 3.8.c and Figure 3.8.d show that for a low *ACH* (0.5 h^{-1}), even without adsorption, a good *TLRF* is achieved (90%), while for a high *ACH* (2 h^{-1}), even with adsorption, the *TLRF* is not so high (85%). This situation confirms the fact that for peak chemicals the greatest toxic load reduction is due to the reduction of the maximum outdoor concentration. Therefore, shelter-in-place will be more effective as lower the *ACH*, and even better if adsorption takes place.

For cumulative substances (n = 1), the *TLRF* decreases as the *ACH* increases. Nevertheless, adsorption lowers the reduction and produces a quick stabilization of the TL_i after the passage of the cloud. From this figure we can also see that if we double the *ACH*, the TL_i for peak substances (n > 1) also doubles its value, while the increase of the TL_i for cumulative substances (n = 1) is lower. Table 3.7 shows the percentage by which the *TLRF* decrease due to the increase of the *ACH*, with regards to the case where *ACH* = 0.5 h^{-1}, assessed at 2 h. From the table we can see that the variation of the *ACH* mainly affects the *TLRF* of cumulative

substances that does not adsorb onto indoor surfaces, and produces decays of 47.5 to 93% on the *TLRF* for *ACH* of 1 and 2 h^{-1} respectively.

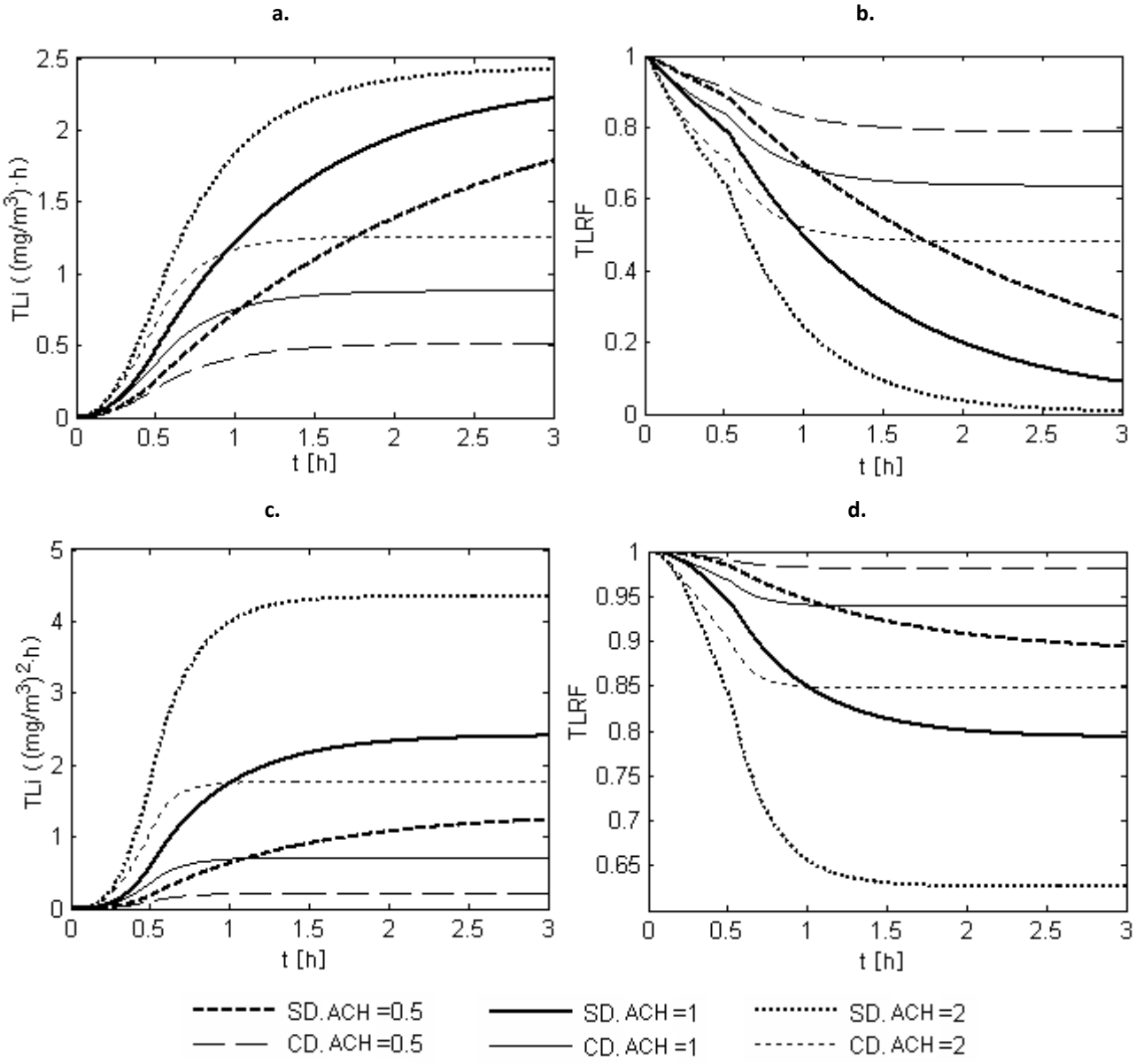

Figure 3.8 Influence of the *ACH* on the TL_i and *TLRF* for *n*=1 (a, b) and *n*=2 (c, d). SD: without adsorption CD: constant adsorption

In relation to the SF_i (see Table 3.7), the variation of the *ACH* influences more this parameter in the case of peak chemicals, for which an increase on the *ACH* produces a higher decay on the SF_i than in cumulative chemicals, as shown in Figure 3.9. This behavior is also affected by the presence or not of adsorption, being the effect larger if the substance adsorbs, since the speed of gas entrance increases while adsorption velocity remains constant.

Table 3.7 Percentage of decay in the *TLRF* and the SF_i in relation to the case when *ACH* = 0.5 at 2 h (%)

	***n* = 1**				***n* = 2**			
	SD		**CD**		**SD**		**CD**	
	***ACH* = 1**	***ACH* = 2**	***ACH* = 1**	***ACH* = 2**	***ACH* = 1**	***ACH* = 2**	***ACH* = 1**	***ACH* = 2**
TLRF	47.5	93	21.5	39	12	31	4	13
SF_i	29	29	42	59.5	32	50	44.5	65

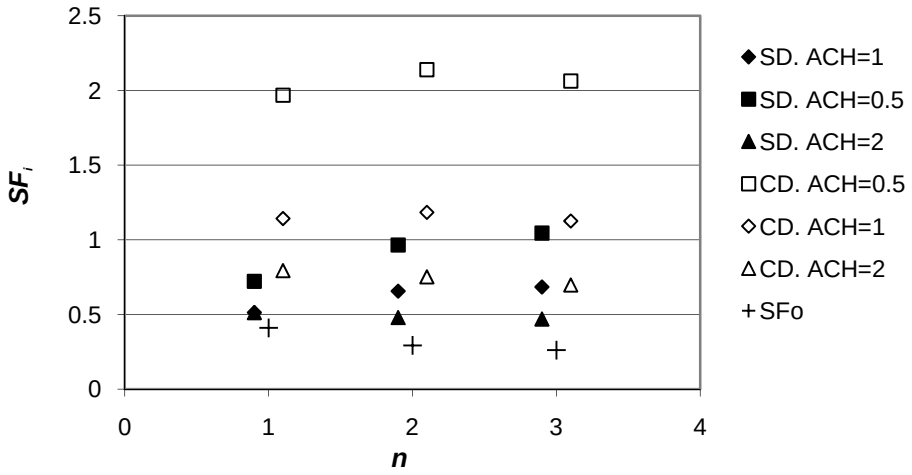

Figure 3.9 Influence of the *ACH* on the SF_i (for a shelter duration of 2 h). SD: without adsorption CD: constant adsorption

Influence of release duration

In this case we want to see the influence that the same quantity of toxic substance can have on the TL_i when released in different lapses of time. For peak substances, lowest TL_i occurred for longer release periods since this case present the smallest peak of C_i (Figure 3.6.c). Even though, the case that presents the smallest TL_i (CD, t_1 = 2 h, Figure 3.10.c) is not the one that has the highest *TLRF*, as might be expected, since the outdoor concentration profile change as well as the TL_o, therefore the *TLRF* also change (Figure 3.10 d). For cumulative substances, the duration of the release has small influence on the TL_i and *TLRF*, as can be seen in Figure 3.10.a and b, where independently of the release duration they tend to the same value.

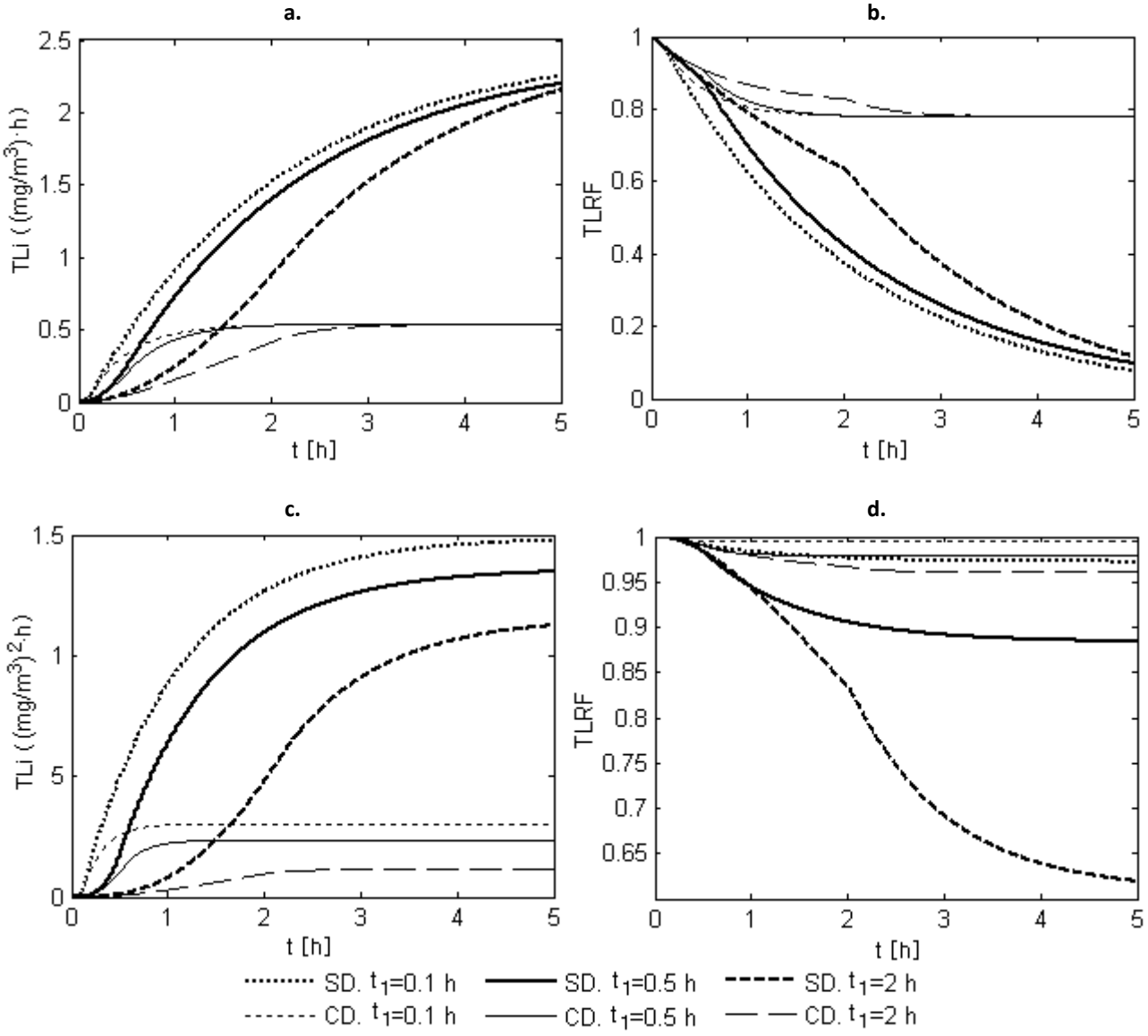

Figure 3.10 Influence of release duration on the TL_i and the *TLRF* for *n*=1 (a, b) and *n*=2 (c, d)

Influence of release magnitude

The magnitude of the release has no effect on the *TLRF*, since its variation influences both outdoor and indoor concentration in the same way (see Figure 3.11 a). However, due to the increase of C_i, TL_i also increases and care should be taken because, although the *TLRF* remains high, the TL_i could reach and exceed the TLL (Figure 3.11 e). For peak chemicals we can observe that the TL_i increases by a factor of 10^6 when the emission changes from 1 to 1000 kg, and by a factor of 10^2 when it changes from 100 to 1000 kg (Figure 3.11 e). For cumulative chemicals the TL_i reached is lower than for peak chemicals (Figure 3.11 b and c).

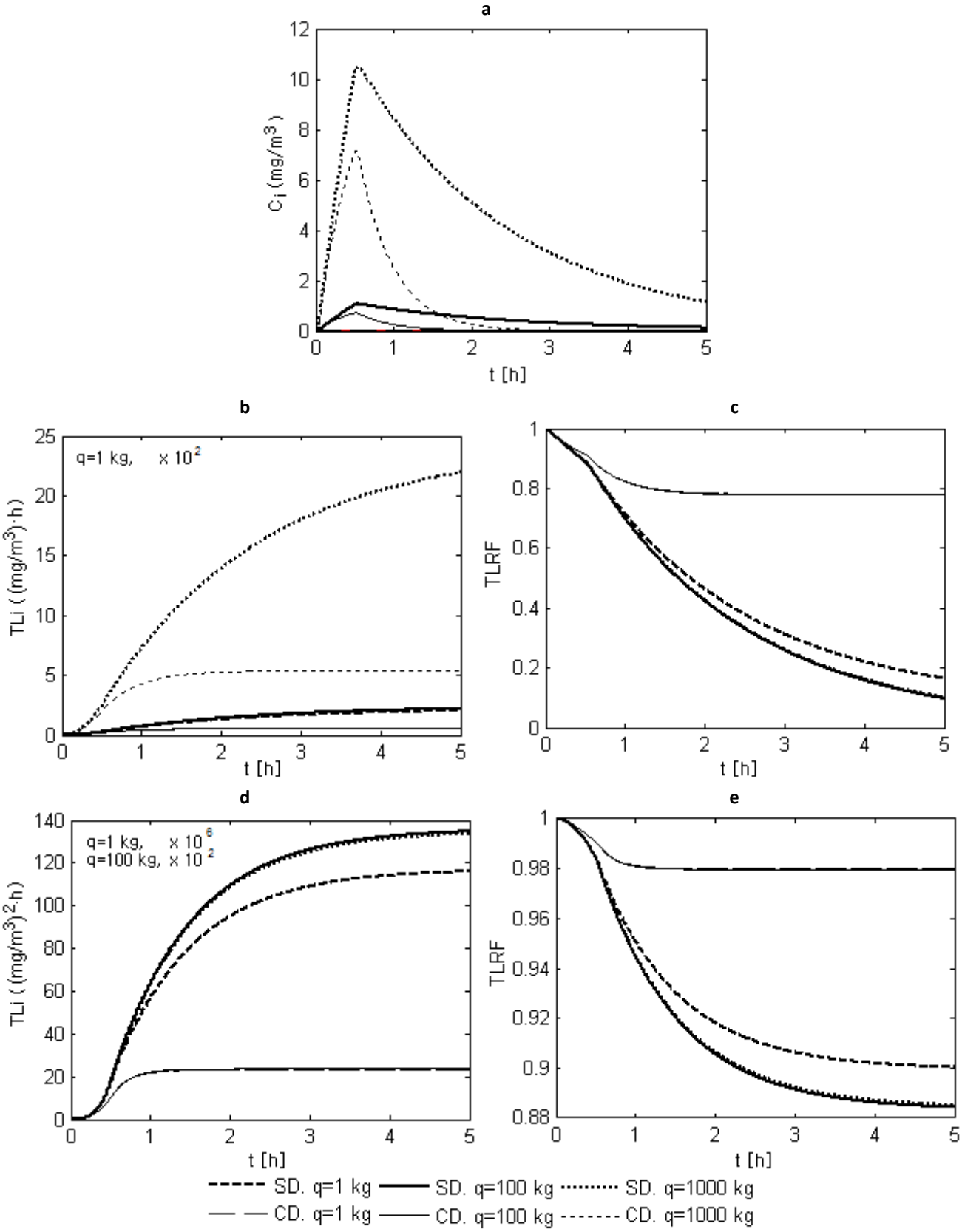

Figure 3.11 Influence of release magnitude on the *TL*$_i$ and the *TLRF* for *n*=1 (b , c) and *n*=2 (d, e)

Influence of atmospheric stability

The atmospheric stability has an important effect on the estimation of outdoor concentration, which consequently affects indoor concentration behavior for the three types of stability assessed. A stable atmosphere causes a higher outdoor concentration followed by neutral and unstable atmospheres (Figure 3.12a). Therefore, assuming a fixed *ACH* as in this case (independent of meteorological conditions), the stable atmosphere leads to the highest TL_i. Concerning the situation whether adsorption takes place or not, an interesting behavior is identified specially for peak chemicals, in which TL_i in stable atmospheres are the highest independently of adsorption, while for cumulative chemicals, the presence of adsorption can lower the TL_i of a stable atmosphere under the TL_i of the neutral atmosphere without adsorption (Figure 3.12.b and d). With regards to the *TLRF*, there is no influence since the variation of atmospheric stability affects outdoor and indoor concentration in the same way.

In terms of the SF_i, Figure 3.13 clearly shows that shelter-in-place is favored by an unstable atmosphere, for which the SF_i increased by a factor of 5 in relation to the neutral atmosphere in both cases, with and without adsorption. In the case of a stable atmosphere, the SF_i decrease by around 45% with regards to the neutral atmosphere in both situations too, with and without adsorption (see Table 3.8). Therefore we can say that independently of the substance and adsorption condition, the change of the atmospheric stability produce an increase on the SF_i by around the same factor for an unstable atmosphere, or a decrease in the case of a stable atmosphere. Nevertheless we should note that we assumed a fixed *ACH*, which actually may vary according to meteorological conditions.

Table 3.8 Percentage of variation of the SF_i with atmospheric stability in relation to the neutral atmosphere at 2 h (%)

	***n* = 1**				***n* = 2**			
	SD		**CD**		**SD**		**CD**	
	Stable	**Unstable**	**Stable**	**Unstable**	**Stable**	**Unstable**	**Stable**	**Unstable**
SF_i	-43*	527	-43	527	-44.5	512	-49	464

* The negative sign denotes a decrease on the SF_i

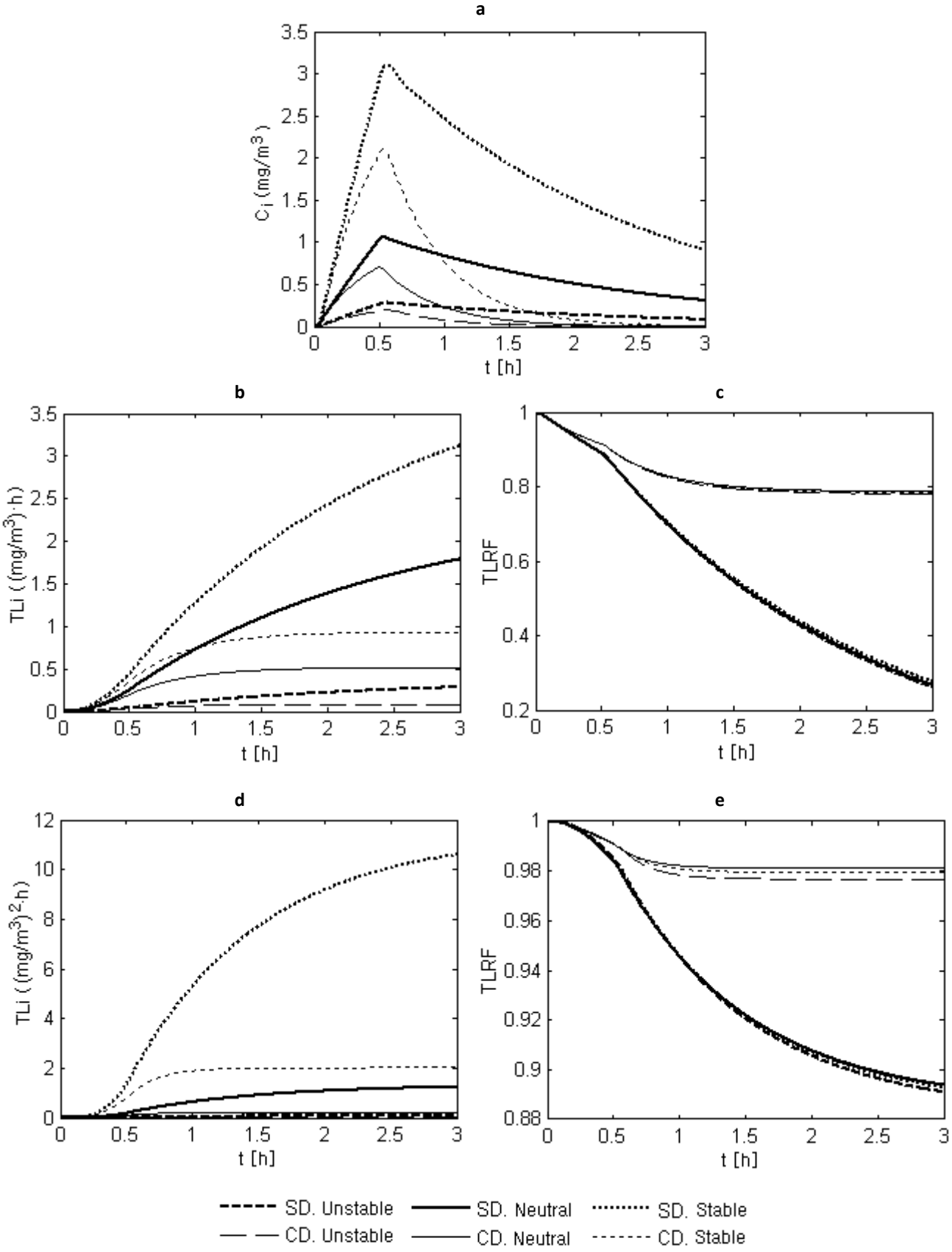

Figure 3.12 Influence of atmospheric stability on the TL_i and the *TLRF* for n=1 (b, c) and n=2 (d, e)

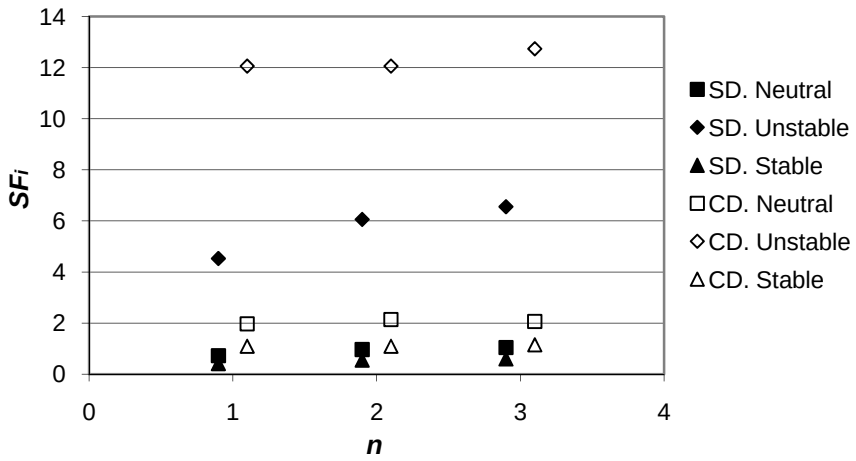

Figure 3.13 Influence of atmospheric stability on the SF_i (for a shelter duration of 2 h)

3.2.2 Based on the evacuation radius: analysis of the Catalan methodology

In order to analyze the performance of the Catalan government methodology to determine the evacuation radius in the event of a toxic gas release (described in section 2.5), we introduced some variations in relation to the *ACH* used, and the way of estimating *Ci* and *TLi*. We took into account the mathematical models described in section 2.2 to calculate indoor concentration (involving sorption into indoor surfaces), and we also developed a parallel analysis to assess the effectiveness of shelter-in-place, based on the AEGL-3, in order to compare the results and confirm the fact that 0.1% casualties are expected indoors. Thereby 4 methodologies are evaluated: the method used by Catalan government (method 1), the same methodology but reducing the *ACH* used (method 2), and two modifications of method 2 changing the way of estimating C_i, without sorption (method 3) and with sorption (method 4). An analysis of the response behaviour due to external conditions like substance type and atmospheric stability was also made.

Methods 3 and 4 differ from the first one specially in the way of estimating C_i. In method 3, the model without adsorption is used (Eq. 2.22), while the constant adsorption (Eq. 2.23) is used within method 4. Method 2 instead, only differs with method 1 in the *ACH*, which is assumed as 1 h^{-1}, since from the experimental data reviewed in section 2.4.4 this is a more typical value of *ACH* among single-family dwellings than 2 h^{-1}. The estimation of *TL*, *Pr* and *P* in these methods is computed using Eq. 1.1, Eq. 2.2 and Eq. 2.3, respectively. Table 3.9 summarized the parameters used in the four methods.

Table 3.9 Parameters used in the four methodologies to estimate the evacuation radius

Parameter	Method 1 (M1)	Method 2 (M2)	Method 3 (M3)	Method 4 (M4)
ACH (h^{-1})	2	1	1	1
C_i	Eq. 2.59	Eq. 2.59	Eq. 2.22	Eq. 2.23
TL_o	$C_o^n \cdot t$	$C_o^n \cdot t$	$\int_0^t C_o^n dt$	$\int_0^t C_o^n dt$
TL_i	$C_i^n \cdot t$	$C_i^n \cdot t$	$\int_0^t C_i^n dt$	$\int_0^t C_i^n dt$

Indicators used to assess shelter-in-place effectiveness were the *TLRF*, the *SF* and the *SFM*. To estimate SF_i and SF_o, we chose as TLL the AEGL-3 at 30 min, since it represents a concentration above which general population, including susceptible individuals, could experience life-threatening health effects or death, and therefore can be used as a reference to compare the evacuation radius.

The case study used to carry out the analysis comprises an emission source at a ground level that lasts for half an hour, at a rate of 0.555 kg·s^{-1} (1000 kg). The dispersion of the toxic cloud was computed downwind using the Gaussian dispersion model (Eq. 2.31 and Eq. 2.32), at a height of 2 m, neutral stability, wind speed of 4 m·s^{-1}, and a terrain ground roughness of 1 m (corresponding to urban or industrial areas). For methods 1 and 2, the evacuation radius and the indicators of shelter-in-place effectiveness were estimated for 30 minutes of sheltering (equal to the emission duration). In the case of methods 3 and 4 for which the time is considered from the beginning of the release, the calculations were performed from the beginning of the release until it is safe to exit the shelter, it is when C_o decreases and therefore C_i becomes larger than C_o. For these methods the calculation time is larger, however, it should be noted that C_o would remain as 0 until the cloud reached the place, and then C_i would increase until the cloud has passed, which would be approximately the same time that the emission duration. For method 4, where adsorption over indoor surfaces is considered, the *A/V* relation was taken as 3.5 m^{-1} and v_d as $1 \cdot 10^{-4}$ m·s^{-1}, like in the previous section.

Substances selected for the analysis were chlorine (Cl_2), methyl isocyanate (Iso), acroleine (Acro), hydrogen fluoride (HF) and mustard gas (MG). These substances were selected due to their toxicity and because they have different values of *n*, so the behaviour of this parameter can be studied. To assess the influence of this parameter on the estimation of the evacuation

radius, it was varied between 0.5 and 3 for isocyanate, acroleine and mustard gas, and the corresponding evacuation distances were obtained. Table 3.10 shows the Probit constants and the AEGL-3 for these substances. Probit constants for mustard gas were estimated from lethal dosages (LC_{50} and LC_{01}) reported by Hartman (2002) fixing n = 2, since the constants included within the Serida Database for this substance correspond to the default values (Espinar, 2005), leading to an overestimation of the evacuation radius.

Table 3.10 Toxic parameters of the substances

Substance	A[1]	B[1]	n[1]	AEGL-3 30 min mg/m^3 (ppm)[2]
Cl_2	-6.35	0.50	2.75	81.194 (28)
Iso	-1.20	1.00	0.70	0.933 (0.4)
Acro	-4.10	1.00	1.00	5.732 (2.5)
HF	-8.40	1.00	1.50	50.715 (62)
MG	-5.47[3]	1.10[3]	2.00	2.700 (0.41)

[1] Constants taken from Serida Database 1.3 (1999), concentrations must be in mg/m^3 and time in min.
[2] Values taken from EPA (http://www.epa.gov/oppt/aegl/pubs-/results56.htm)
[3] Values estimated from lethal dosages Hartman (2002)

Behaviour of the evacuation radius

Table 3.11 shows the evacuation radiuses estimated with the four methodologies for each substance. Distances obtained with M1 were the highest while those obtained with M4 were the lowest distances, as it was expected since M1 considers a higher *ACH*, and M4 takes into account adsorption over indoor surfaces in the estimation of C_i. With regards to M2 and M3, which consider similar assumptions, the results born out the fact that M2 predicts lower distances than M3 for substances with $n > 1$ (increasing the difference with the increase of n), while for substances with n closer to 1 the evacuation radiuses predicted were almost the same; as previously discussed in section 2.5. However, although distances predicted with M2 for peak substances (n >1) underestimate distances obtained with M3, they were very similar to those predicted with M4 and remained above them.

We can also see that SF_o stay under 1 in all cases, as should be since the *TLL* is supposed to be exceeded outside and thus sheltering or evacuation should be implemented. Since the TL_i must be the same to match the evacuation criteria (P = 0.001), the SF_i is the same by substance independently of the method, as presented in Table 3.11. This parameter is also expected to

be equal or lower than one, as from the AEGL-3 definition no one would be in risk of death if this threshold value is not exceeded. However the SF_i for methyl isocyanate is higher than one, showing some discrepancy between the Probit and the AEGL-3 criteria. Concerning the *TLRF*, a trend within *n* can be identified where higher *TLRF* belong to the substances with higher *n*, which born out the fact that sheltering is more effective in the case of peak chemicals than in cumulative chemicals, as discussed before.

Table 3.11 Evacuation radius estimated with different methodologies

Substance	Method	Evacuation Radius (m)	TLL	SF_o	SF_i	*SFM*	*TLRF*	P_o (%)	P_i (%)
Chlorine	M1	203	5.35E+06	0.252	0.68	2.718	0.936	4.40	0.10
	M2	149		0.147		4.693	0.985	16.6	
	M3	164		0.175		3.938	0.977	11.4	
	M4	147		0.144		4.797	0.986	17.4	
Methyl isocyanate	M1	4695	28.587	0.521	1.41	2.718	0.503	0.8	0.10
	M2	3300		0.302		4.693	0.661	2.2	
	M3	3294		0.295		4.799	0.666	2.3	
	M4	3005		0.253		5.595	0.700	3.0	
Acroleine	M1	716	171.96	0.155	0.42	2.718	0.632	1.8	0.10
	M2	518		0.089		4.693	0.786	6.2	
	M3	524		0.090		4.632	0.784	6.0	
	M4	471		0.075		5.602	0.821	8.6	
Hydrogen Fluoride	M1	223	10835	0.185	0.50	2.718	0.776	5.70	0.10
	M2	163		0.107		4.693	0.901	22.3	
	M3	169		0.115		4.367	0.890	19.4	
	M4	152		0.095		5.280	0.917	27.9	
Mustard gas	M1	1280	218.7	0.192	0.52	2.718	0.864	18.1	0.10
	M2	910		0.110		4.693	0.954	62.8	
	M3	996		0.128		4.123	0.941	48.8	
	M4	880		0.104		4.956	0.959	66.6	

The behaviour of *P* and *SF* with distance shows that *P* always decreases with distance while the *SF* increases (e.g see acroleine in Figure 3.14). There is also a big difference between P_o and P_i estimated with all the methods, which assures that an important toxic load reduction is achieved within shelter. For all substances, the P_i and the SF_i estimated with M4 are the lowest and the highest, respectively; while the results obtained with M1 were the opposite. In the case of M3 and M2 the behaviour of the *SFi* and the *P* is the same, as the *n* for the acrolein is 1.

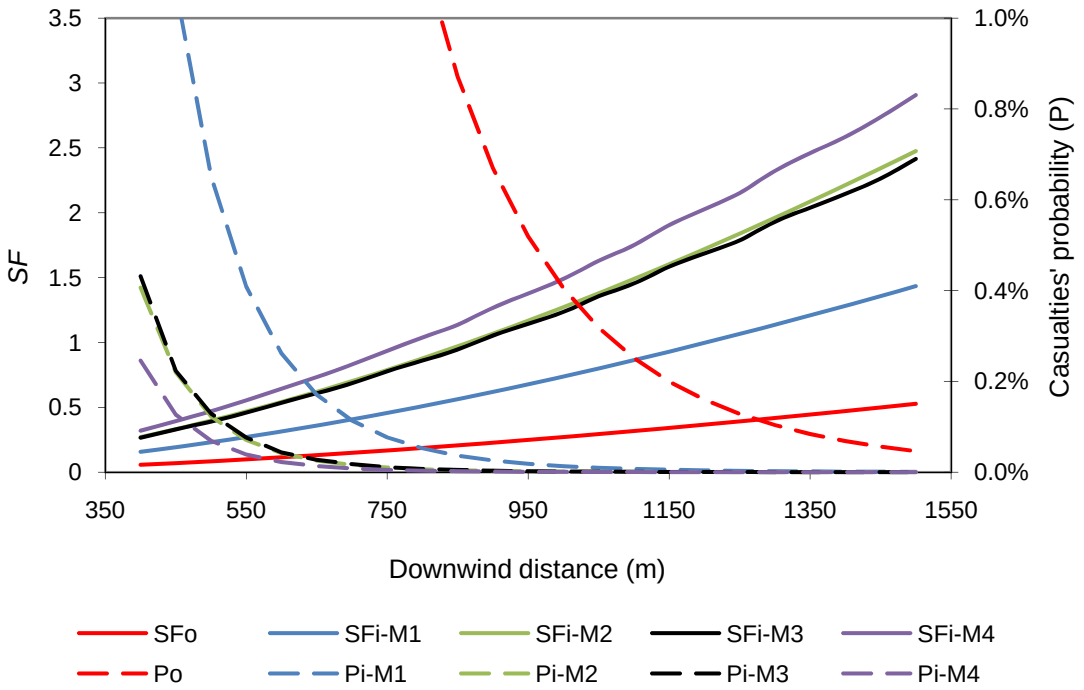

Figure 3.14 Behaviour of casualties' probability and safety factors with distance for acroleine

Variation of the evacuation radius as a function of *n* for acroleine, methyl isocyanate and mustard gas are presented in Figure 3.15. Two behaviours can be identified, one in which the distance increases with *n* and the other in which it decreases. The first case takes place when the concentration needed to reach the TL_i that satisfies the Probit function for a defined probability is higher than 1 mg/m^3 (e.g. acroleine and mustard gas); in that case, the evacuation radius increase with *n***.** The second situation takes place when the above mentioned concentration is less than 1 mg/m^3 (e.g. isocyanate), then, the evacuation radius decrease with *n*. Particularly, methyl isocyanate follows the second behaviour, since it is necessary that indoor concentration stay below 1 mg/m^3 to reach a TL_i of 22.4 (mg/m^3)$^{0.7}$ min, which is the one required by the Probit analysis to have a probability of 0.1%. Such low concentrations (< 1 mg/m^3) would only be needed when dealing with a really high toxic substance. From this figure we can also see that the difference between the radiuses estimated with M2 and M3 increase with *n*.

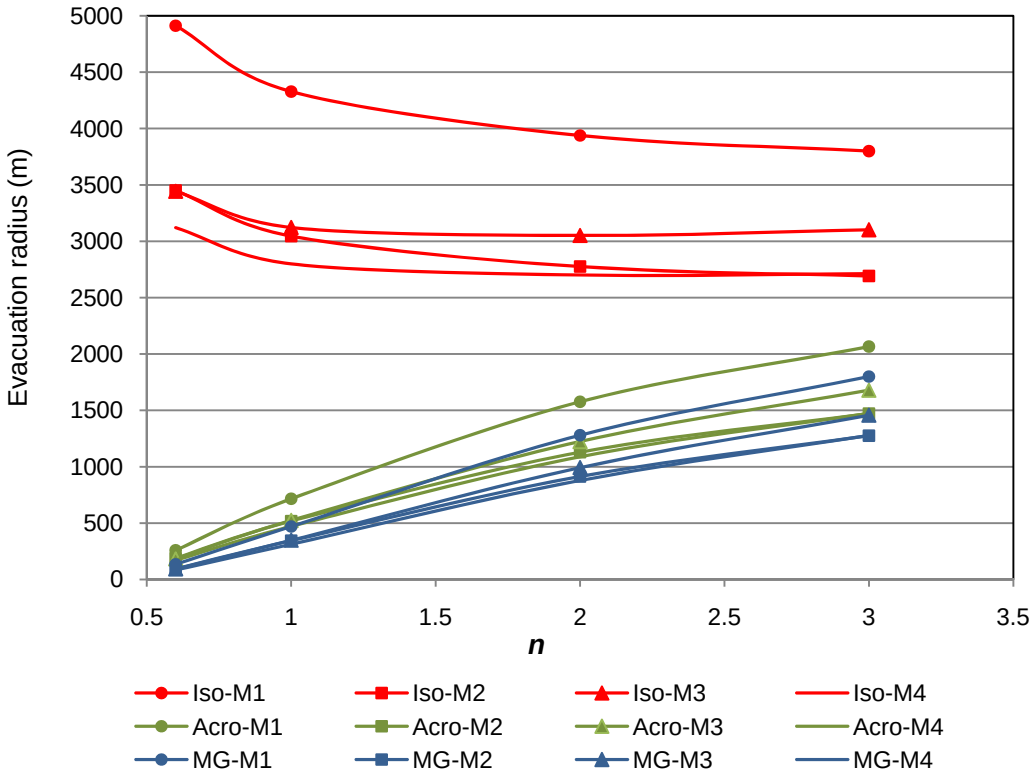

Figure 3.15 Variation of the evacuation radius with *n* for a sheltering time of 30 min

Concerning the meteorology, atmospheric stability and wind speed, the evacuation radius obtained for more stable atmospheres (class E, 3 m/s) are larger than the distances obtained in a neutral atmosphere (class D, 3 m/s), while the radius obtained in a more unstable atmosphere (class B, 3 m/s) is smaller, like half the distance in a neutral atmosphere, as presented in Figure 3.16 for acroleine. In relation to the wind speed, larger distances are predicted for lower wind speeds. These behaviours are due to the quick dispersion and turbulence present in an unstable atmosphere, and higher wind speeds, which makes that the toxic substance disperses better and faster. However, the *ACH* is not a constant value, and it changes with wind speed, therefore, this comparison concerning the meteorology should also take into account the effect of the wind speed over the *ACH*. Since, as reported by Guyot *et al*. (2008), although the pollutant dilutes faster with increasing wind speed, the resulting dose inside the shelter could increase due to the effect of the wind over the *ACH*, accelerating the toxic gas transfer to the indoor.

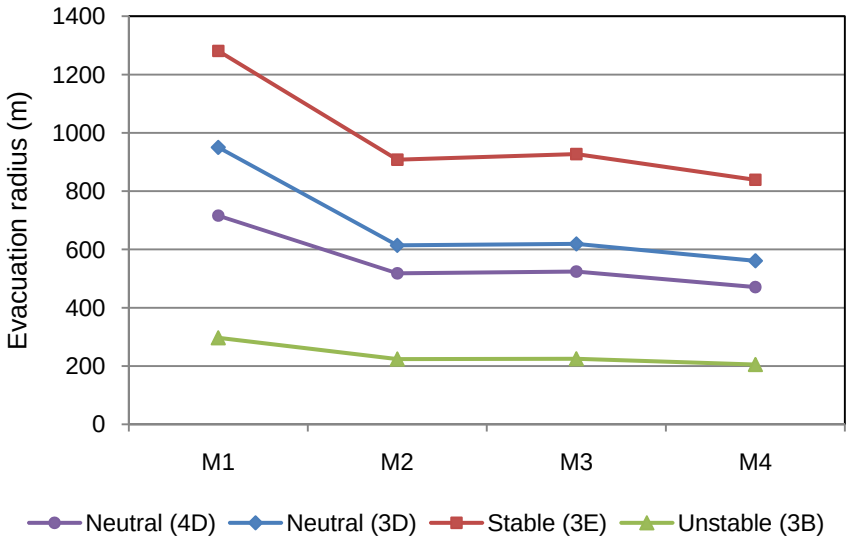

Figure 3.16 Variation of the evacuation radius with atmospheric stability for acrolein

Therefore, one of the most important limitations identified in this chapter when assessing the indoor concentration is the lack of knowledge about the *ACH*, which, as seen with methods 1 and 2, is a very important parameter that conditions the evacuations radius obtained (an increase of the *ACH* by a factor of 2, leads to an increase in the evacuation radius of 35%). In addition, at a community scale every building will present a different *ACH* regarding its characteristics and meteorological conditions, and the assumption of a fixed value could lead to under or overestimations of the evacuation distances.

In general, the methodology used by the Catalan government gave similar estimations to those of method 3 when the value of *n* is around 1, while for substances with higher values of *n*, the Catalan methodology tends to underestimate the evacuation radius obtained with method 3 and therefore care should be taken when using it with peak substances. Even though, in the case of a toxic release the substance is already known and thereby an adequate model can be selected by emergency managers to estimate C_i and TL_i, then, the greatest concern becomes the estimation of the *ACH*. An approximation of the *ACH* is needed and should be implemented in order to better represent the real situation.

For the substances studied, method 3 was the one that predicted the lowest evacuation radius and the highest safety factor for the same distance; the other methods gave more conservative results. From a theoretical point of view, method 3 is also the most rigorous, since it incorporates an indoor concentration model that takes into account deposition over

indoor surfaces, and assesses the toxic load according to the profile of the indoor concentration. Therefore, this methodology should be the one that better represents the reality. Even though, since there is not experimental data available to validate the results obtained with the four methods, a final statement could not be given.